

REMARKS

Interview

Applicant wishes to express its appreciation for the courtesy shown to applicant's representative in the recent telephone interview.

In the interview, the Examiner identified two technical issues:

1. Do the terms "natural" and "synthetic" quartz glass as used in the claims have a meaning and distinction that is commonly understood by those of skill in the art; and
2. Is it possible to make bubble-free natural silica glass.

Subject to establishing these two technical issues, the Examiner agreed that the claims as presently formulated distinguish over the cited prior art.

Two articles are appended that show that the terms "natural" and "synthetic" quartz glass have clear and distinct meanings in the art, and that natural quartz glass can be formed without bubbles.

Natural and Synthetic Quartz Glass

The claims herein make reference to "naturally occurring quartz glass" and "synthetic quartz glass".

The specification clearly defines these materials. "Synthetic quartz glass" is glass formed from synthetic silica powder. See, Specification, page 8, lines 5 to 19 ("Subsequently, a synthetic silica powder is supplied to the high temperature atmosphere 15 from the silica powder supply nozzle 14, and, on forming a quartz glass layer (first part 5) at the desired position by melting and vitrifying the thus supplied silica powder, thereby forming a synthetic

quartz glass inner layer 5 ...”). “Naturally occurring quartz glass” is quartz glass that is formed from naturally occurring quartz glass powder. See, Specification, page 8, lines 12 to 14 (“In the same way and by using naturally occurring quartz glass powder, a second part 6 of the inner is formed on the wall in a range from 0.5 H to 0.8 H consisting of naturally occurring quartz glass layer.”)

The terms “synthetic silica” and “natural silica” are common terms in the art. For example, in the attached article, P. Geittner et al., “Hybrid Technology for Large SM Fiber Preforms”, compares three types of silica tubes, natural silica and two samples of synthetic silica, exemplifying use of these terms in the art.

Referring to the attached page from Wikipedia, the entry under “Fused Quartz”, the section states that fused quartz is manufactured by melting naturally occurring quartz crystals of high purity at 2000 degrees C. “Synthetic fused silica” is made from a continuous flame hydrolysis process that involves gasification of a silicon-rich chemical precursor. See Wikipedia attachment, page 1.

It is therefore apparent that there is an art-recognized distinction between the natural material, i.e., naturally occurring quartz silica, and synthetic material derived from chemical processes that produce the silica material.

Differences between natural and synthetic silica glasses are discussed in detail in the attached article of R. Brückner, “Properties and Structure of Vitreous Silica”. Brückner lists four types of silica glasses on page 124. Types I and II are made from natural quartz by electrical or flame fusion. Types III and IV are made from hydrolyzation in an oxygen-hydrogen flame, or from water-free flame processes.

One interesting difference is seen in the transmission curves of the different types, seen in FIG.3 on page 130 of the article, and also in the thermal expansion graphs of FIG. 12 on page 140.

It is clear from the foregoing literature that those of skill in the art would use the terms “naturally occurring quartz glass” and “synthetic quartz glass”, and that those terms identify distinct materials.

Bubble free naturally occurring quartz glass

The Examiner has also asked for a reference that indicates that a transparent quartz glass layer can be of naturally occurring quartz glass.

The attached articles all establish this as well.

Referring to Brückner, FIG. 3, it is apparent that Type I and II silica glasses exhibit a transmission near 100% for light of wavelengths of .25 to 2.5 microns. If there were bubbles in those natural silica glass samples, they would be opaque or translucent and one could not expect transmission anywhere near 100%.

The Wikipedia article on Fused Quartz notes that fused quartz (made from naturally occurring quartz crystals) is “normally transparent”. See page 1, line 19.

Geittner et al. relates to fiber preforms. Geittner proposes making the core of the preforms of synthetic glass (CVD, PCVD-made) and the outer parts (jacket tube) of natural silica (see “Conclusions”, page 1453). The last sentence in chapter “Results” (page 1453) mentions “tubes from natural silica”, which is the low-cost silica glass. Geittner would not propose “tubes from natural silica” if these tubes were porous and contained bubbles. Porous tubes could not be converted to fiber.

Therefore it is clear that naturally occurring quartz glass can be transparent.

Amendment to Specification

It was noted that a line of text was out of place in the specification, and the present amendment shifts it to its proper location four lines higher.

Double patenting rejection

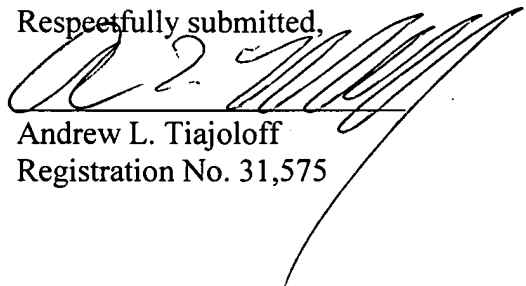
Attorney for applicant submits herewith terminal disclaimers by each owner of the present application for any part of the term of a patent to issue on the present application that would extend beyond the end of the term of any patent that may issue on 10/555,853. A check including the amount of \$240.00 for the fees for two disclaimers is submitted herewith. If the check is insufficient or not found, please deduct any fee that may be required from deposit account no. 501659.

It is believed that all of the technical issues raised by the Examiner have been resolved by the materials submitted herewith, and formal allowance is therefore respectfully requested. Should any questions arise, the Patent Office is invited to telephone attorney for applicants at 212-490-3285.

Tiajolloff & Kelly LLP
Chrysler Building, 37th floor
405 Lexington Avenue
New York, NY 10174

tel. 212-490-3285
fax 212-490-3295

Respectfully submitted,



Andrew L. Tiajolloff
Registration No. 31,575

perform

Hybrid Technology for Large SM Fiber Preforms

**P. Geittner
H.-J. Hagemann
H. Lydtin
J. Warnier**

**Reprinted from
JOURNAL OF LIGHTWAVE TECHNOLOGY
Vol. 6, No. 10, October 1988**

Hybrid Technology for Large SM Fiber Preforms

P. GEITTNER, H.-J. HAGEMANN, H. LYDTIN, AND J. WARNIER

Abstract—A hybrid technology has been developed for the preparation of standard and dispersion-modified single-mode (SM) fibers. Only the most important central region of the fibers is prepared by plasma-activated chemical vapor deposition (PCVD). The optical cladding is added by substrate and jacket tubes obtained from low-cost shaping and sintering technologies. Due to *in situ* plasma etching, no disturbance is caused by the interfaces. Low attenuation is achieved with less than 5 percent of the fiber volume made by PCVD (core region). The hybrid technology allows economic mass production of preforms containing more than 300 km of fiber.

INTRODUCTION

THE DEMAND for optical fibers is expected to grow by several orders of magnitude with the future installation of fiber optic subscriber loops and if the prices can be significantly lowered. This might require a revision of the established fiber production technologies to allow cheap mass production with quality standards similar to those of today's telecommunication fibers.

A drawback of the existing technologies is that the core and all of the optical cladding of single-mode (SM) fibers is fabricated by elaborate CVD methods with optimum optical quality, whereas the actual requirements are only very high for the core but can be weakened drastically in the cladding with increasing distance from the center of the fiber.

This is illustrated in Fig. 1 which gives a rough impression of the rapid decrease of the light intensity outside a given diameter in the cladding of a SM fiber [1].

Here we propose a hybrid concept for the fabrication of SM fibers which allows this radial dependence to be taken into account by using different materials and preparation technologies in different regions of the preform. The main feature of the hybrid technology is that essentially only the core material is prepared by CVD, and the remaining optical cladding is added by the substrate tube and jacketing techniques using synthetic silica tubes made from low-cost SiO_2 raw materials by fast shaping and sintering processes.

We have been able to demonstrate the feasibility of the hybrid concept by preparing low attenuation SM fibers which consist of only a small fraction of CVD material, and most of the optical cladding provided by prefabricated synthetic silica tubes.

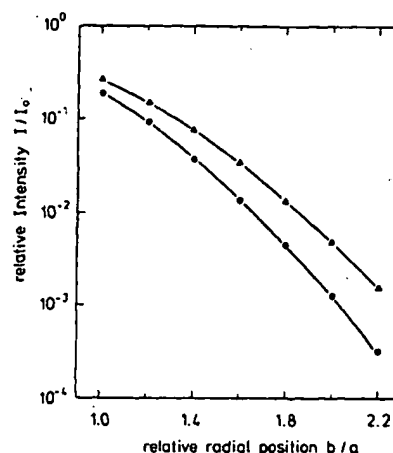


Fig. 1. Calculated fraction of the light intensity (Gaussian approximation) outside a given radius b as function of the ratio b/a at 1300 nm (●) and 1550 nm (▲) (core radius $a = 4.2 \mu\text{m}$, $\Delta = 0.3$ percent).

THE HYBRID CONCEPT

The hybrid concept is illustrated in Fig. 2. Only the core material of the SM fiber (α) is deposited by plasma-activated chemical vapor deposition (PCVD) [2] in thin-walled substrate tubes made of very high purity synthetic silica (β_1). The coated tube is collapsed to a rod containing approximately only 5 percent of the final fiber volume. The major part of the optical cladding is added as high purity jacket tube (β_2). The overcladding is accomplished by normal "rod-in-tube" (RIT) techniques with silica tubes of well-defined geometric tolerances (γ).

This hybrid concept allows the convenient preparation of very large preforms as needed for future economic mass production. To fabricate, for example, an 8-kg preform containing 300 km of step index SM fiber, only 50 g of PCVD material are necessary for the core material, and only 150 g must be collapsed yielding, e.g., a central rod 10 mm in diameter and 1 m in length. The corresponding figures for a dispersion flattened SM fiber [3] are 150 g of PCVD material and 300 g to be collapsed.

In Table I an example for parameters of a conventional PCVD process and of the hybrid technology are compared for a fiber length per preform of 50 and 300 km, respectively. The PCVD collapsing and RIT steps are characterized by the fiber regions involved (α , β , β_1 , γ_1 , or γ_2), their relative fraction of the total fiber volume, and the deposition and collapsing rates that would be necessary for a balanced fabrication.

A further comparison is made in Table II. It is assumed

Manuscript received January 29, 1988; revised May 6, 1988.
The authors are with Phillips GmbH Forschungslaboratorium Aachen, 5100 Aachen, West Germany.
IEEE Log Number 8822709.

TABLE I
COMPARISON OF SOME TYPICAL PARAMETERS OF THE PRESENT
CONVENTIONAL PCVD TECHNOLOGY AND OF THE HYBRID TECHNOLOGY

		PCVD	Collapsing	RIT
<u>Present Technology</u>	regions affected	α, β	α, β, γ	γ_2
typical fibre length 50 km	volume fraction	25%	50%	50%
	typical rates	1g/min	2g/min	-
<u>Hybrid Technology</u>	regions affected	α	β_1	β_2, γ
typical fibre length 300 km	volume fraction	2.5%	5%	95%
	typical rates	0.5g/min	1g/min	-

TABLE II
EXAMPLE FOR GEOMETRIC DIMENSIONS AND PROCESSING TIMES OF 1-m
PERFORMS FOR 160 km OF SM FIBERS

	Present Techn.	Hybrid Techn.
Substrate tube diameter	35 mm	17 mm
Preform diameter	29 mm	9 mm
Cladding tube diameter	-	25 mm
Cladding tube wall thickness	-	7 mm
PCVD deposition rate	3g/min	0.5g/min
Deposition time/pref. length	5min/cm	0.6min/cm
Collapsing time/pref. length	15min/cm	1min/cm
Total processing time	30 h	3h

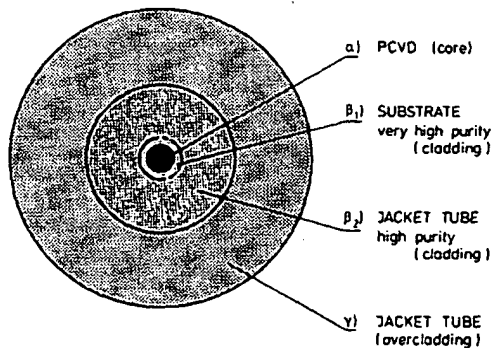


Fig. 2. Hybrid concept: core, cladding, and overcladding regions of a hybrid technology SM fiber.

that 160 km of SM fiber were to be drawn from a preform 1 m in length. Typical tube and preform diameters and characteristic processing data for deposition and collapsing are listed. It is illustrated in Table II that the hybrid technology allows a convenient choice of the major process variables if large preforms are to be prepared.

The introduction of this hybrid concept as a fabrication technology requires the availability of high purity silica tubes, the ability to smooth and clean the optically sen-

sitive surfaces, and the possibility of preparing a central preform rod without bulk contamination from the collapsing procedure.

INTERFACE

To check the influence of exposed surfaces and interfaces in the vicinity of the core, SiO_2 substrate tubes were made by PCVD which were cut, handled, and prepared for deposition as usual. Inside the tubes only core material was deposited. With respect to the interface between the PCVD core material and the "substrate tube" this procedure simulates the preparation of SM fibers by the hybrid technology. Prior to the deposition various surface treatments were tested. The preforms were collapsed, SM fibers were drawn, and the fiber attenuation was measured.

The influence of different heating and etching treatments on the attenuation at 1300 nm is shown in Fig. 3. The reference substrate tube treatment which consists of weak wet chemical etching, rinsing, and drying leaves the interface contaminated (treatment 0). If, in addition, annealing at different temperatures (treatments 1, 2) or *in situ* gas phase etching procedures (treatments 3-5) are

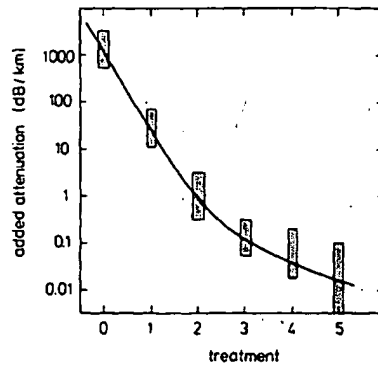


Fig. 3. Attenuation at 1300 nm added by the core-cladding interface for different heating and etching treatments, trace 0: reference; traces 1, 2: additional annealing at $T < 1000^\circ\text{C}$; traces 3-5: additional *in situ* gas phase etching. The substrate tube is of CVD quality.

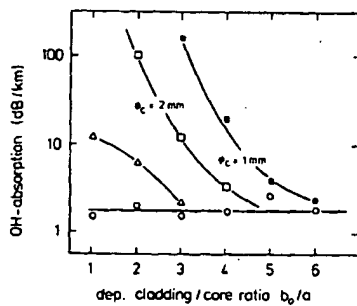


Fig. 4. OH absorption at 1385 nm as a function of the deposited cladding; substrate tubes: ■ natural silica, core diameter of the preform $\phi_c = 1$ mm; □ natural silica, $\phi_c = 2$ mm; △ synthetic silica 1; ○ synthetic silica 2.

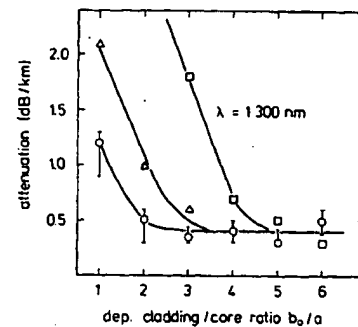


Fig. 5. As Fig. 4, but total attenuation at 1300 nm.

conducted prior to the deposition of the core material, a lowering of the attenuation is achieved.

RESULTS

Three types of silica tubes with different OH content¹ were available which were used as substrate tubes for the deposition (PCVD) of core and cladding material. The ratio of the total PCVD material to the core material was varied between 36 and 1, i.e., ratios of the deposited cladding radius b_0 to the core radius a of 6 to 1 ($b_0/a = 1$ means deposition of core material only). Prior to deposition the inner surface of the tubes was cleaned as described above in order to avoid attenuation from the interface between deposit and substrate.

On lowering the b_0/a ratio, an increase of the 1385 nm absorption indicates OH impurities from the substrate tubes (Fig. 4). Using tubes of synthetic silica 1 the OH absorption increases to ≈ 10 dB/km for $b_0/a < 2$, whereas with tubes of synthetic silica 2 no additional OH absorption occurs. However, high OH absorption peaks appear upon lowering b_0/a using tubes from natural silica.

¹Natural silica, ≈ 150 ppm OH; synthetic silica 1, ≈ 0.3 ppm OH; synthetic silica 2, < 50 ppb OH.

It is noteworthy that the absorption is weaker for preforms with diameters of 2 mm (Fig. 4), since the diffusion lengths (during collapsing and drawing) towards the center remain nearly constant. Thus, mobile impurities are more disadvantageous in the hybrid technology than those with small diffusion coefficients.

First results of the total attenuation at 1300 nm are presented in Fig. 5. With the best synthetic tubes the added absorption is below 0.2 dB/km at $b_0/a = 2$ and below 0.6 dB/km at $b_0/a = 1$. Finally, in Fig. 6 the attenuation spectrum of a hybrid technology SM fiber is shown.

CONCLUSIONS

A hybrid technology has been developed which utilizes different technologies for the preparation of the central core, the optical cladding, and the nonlight-guiding overcladding (Fig. 1). Only the most important core material with its structured refractive index is made by PCVD whereas the cladding is added by substrate and jacket tubes made from low-cost SiO_2 raw materials by fast shaping and sintering techniques.

So far a major obstacle to such an approach had been the disturbance from interfaces within the light-guiding region. This could be solved by the development of an *in situ* gas phase etching.

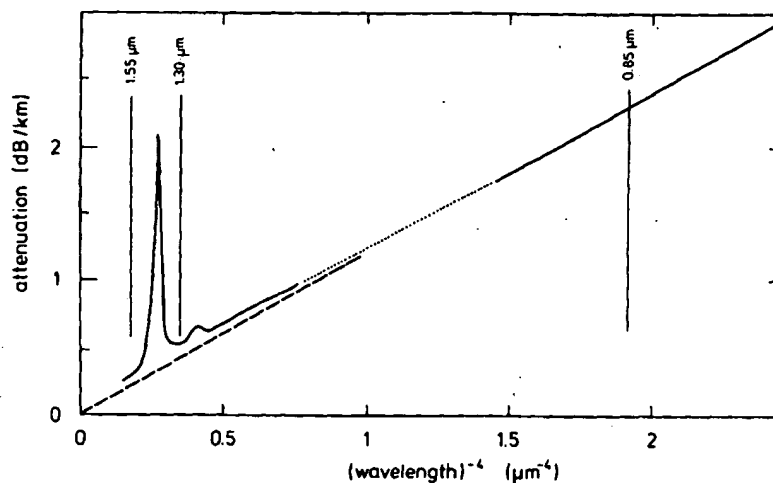


Fig. 6. Attenuation spectrum of a SM fiber prepared by hybrid technology, $b_0/a = 2$. The substrate tube is of synthetic silica 2.

The feasibility has been proven of an advanced hybrid technology to produce low attenuation SM fibers which contain less than 5 percent CVD material. The hybrid technology is appropriate for large preforms containing several hundred kilometers of fiber. It is not restricted to step index profiles but is equally suited for all types of dispersion modified SM fibers.

REFERENCES

- [1] D. Marcuse, "Gaussian approximation of the fundamental modes of graded index fibers," *J. Opt. Soc. Amer.*, vol. 68, pp. 103-109, 1978.
- [2] P. Geittner, D. Küppers, and H. Lydtin, "Low-loss optical fibers prepared by plasma-activated chemical vapor deposition (CVD)," *Appl. Phys. Lett.*, vol. 28, pp. 645-646, 1976.
- [3] P. Bachmann, P. Geittner, and H. Lydtin, "Progress in the PCVD process," in *OFC Tech. Dig.*, Atlanta, GA, 1986, pp. 76-78.



Peter Geittner received the M.S. and Ph.D. degrees in physics from the University of Marburg, W. Germany, in 1969 and 1973, respectively. At the university, he worked on atomic spectroscopy, optical pumping, and spin polarization of molecular beams.

In 1974, he joined the Philips GmbH, Research Laboratory, Aachen, where he worked in research on optical characterization, fiber drawing, process technology for fiber preparation, and fundamentals of CVD diagnostics and laser induced CVD.

Since 1980, he has been mainly engaged in research on the PCVD process. In 1985 he was appointed Senior Scientist at the Philips Research Laboratory, Aachen.

Dr. Geittner is a member of the German Physical Society (DPG) and of the European Society (EPS).



Hans-Jürgen Hagemann received the M.A. degree in solid-state physics from the State University of New York at Stony Brook in 1971 while on a Fulbright Fellowship. He received the degree in physics from the University of Hamburg, W. Germany, in 1974, and the Ph.D. degree from the Technical University of Aachen, W. Germany, in 1980.

In 1974 he joined Philips Research Laboratories in Aachen, working on the electronic and dielectric properties of ferroelectrics and polycrystalline oxides for passive electronic devices. From 1982 to 1983, on leave from Philips, he worked at AT&T Bell Laboratories, Murray Hill, NJ, and investigated diffusion phenomena in ceramic materials. Since 1984 he has done research and development on the PCVD process for the preparation of low-loss optical fibers.

Hans Lydtin was born in Berlin, Germany, on August 12, 1934. He received the diploma and doctor's degree from the Technical University in Berlin in 1959 and 1961, respectively.

In 1962 and 1963, he worked at the Rheinisch-Westfälische Technische Hochschule in Aachen, W. Germany. In 1963, he joined the Philips Research Laboratories, Aachen. Since 1971, he has been in charge of the Solid-State Technology Group in which the PCVD process for optical fiber fabrication has been invented and studied.



Jacques Warnier was born in Mesch-Eijsden, Holland, on August 9, 1950. He studied chemical technology at the Higher Technical Institute in Heerlen and received the Ing. degree in 1970.

In 1972 he joined the Philips Research Laboratories in Aachen, W. Germany, and worked on the chemical vapor deposition of several materials. Since 1980 he has been involved in research on optical fibers by means of the PCVD method.

Fused quartz

From Wikipedia, the free encyclopedia
(Redirected from Quartz glass)

Fused quartz and **fused silica** are types of glass containing primarily silica in amorphous (non-crystalline) form. They are manufactured using several different processes. Note that glasses formed by the traditional 'melt-quench' methods (heating the material to melting temperatures, then rapidly cooling to the solid glass phase), are often referred to as 'vitreous', as in 'vitreous silica'. The term 'vitreous' is synonymous with 'glass', when used in the melt-quench context.

Fused quartz is manufactured by melting naturally occurring quartz crystals of high purity at approximately 2000°C, using either an electrically heated furnace (electrically fused) or a gas/oxygen-fuelled furnace (flame fused). Fused quartz is normally transparent.

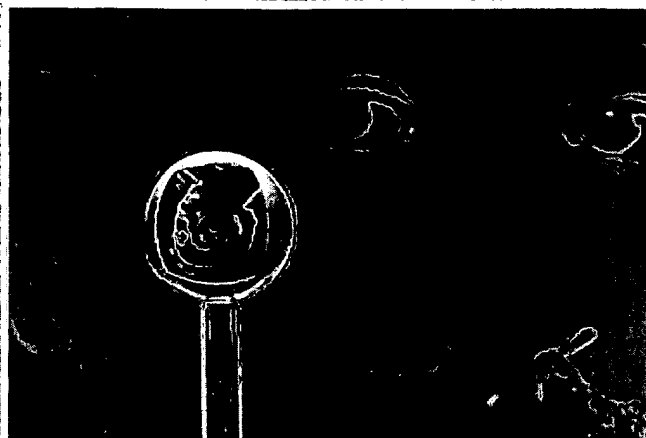
Fused quartz can also form naturally. The naturally occurring form is usually referred to as Metaquartzite and is formed under metamorphic conditions. An increase in heat causes the crystals within the quartz to become fused together.

Fused silica is produced using high purity silica sand as the feedstock, and is normally melted using an electric furnace, resulting in a material that is translucent or opaque. (This opacity is caused by very small air bubbles trapped within the material.)

Synthetic fused silica is made from a silicon-rich chemical precursor usually using a continuous flame hydrolysis process which involves chemical gasification of silicon, oxidation of this gas to silicon dioxide, and thermal fusion of the resulting dust (although there are alternative processes). This results in a transparent glass with an ultra-high purity and improved optical transmission in the deep ultraviolet. One common method involves adding silicon tetrachloride to a hydrogen-oxygen flame, however use of this precursor results in environmentally unfriendly by-products including chlorine and hydrochloric acid. To eliminate these by-products, new processes have been developed using an alternative feedstock, which has also resulted in a higher purity fused silica with further improved deep ultraviolet transmission.

Fumed silica is manufactured by a similar flame hydrolysis process to synthetic fused silica, however it is in the form of a fine powder/dust and is typically used in applications such as fillers for rubbers and plastics, coatings, adhesives, cements, sealants, cosmetics, pharmaceuticals, inks and abrasives.

The optical and thermal properties are superior to those of other types of glass due to its purity (or rather, its lack of impurities). For these reasons, it finds use in situations such as semiconductor fabrication and laboratory equipment. It has better ultraviolet transmission than most other glasses, and so is used to make lenses and other optics for the ultraviolet spectrum. Its low coefficient of thermal expansion also makes it a useful material for precision mirror substrates.



A sphere manufactured by NASA out of fused quartz for use in a gyroscope in the Gravity Probe B experiment. It is one of the most accurate spheres ever created by humans, differing in shape from a perfect sphere by no more than 40 atoms of thickness. It is thought that only neutron stars are smoother.

Contents

- 1 Chemistry
- 2 Applications
- 3 Physical properties
- 4 Optical properties
- 5 Typical properties of clear fused silica
- 6 See also
- 7 External links
- 8 References

Chemistry

Fused quartz is a noncrystalline form of silicon dioxide (SiO_2), which is also called *silica*. (The crystalline form of this material is quartz).

Applications

Specially prepared fused silica is also the key starting material used to make optical fiber for telecommunications.

Because of its strength and high melting point (compared to ordinary glass), fused silica is used as the envelope of halogen lamp, which must operate at a high envelope temperature to achieve their combination of high brightness and long life.

The combination of strength, thermal stability, and UV transparency makes it an excellent substrate for projection masks for photolithography.

Due to the thermal stability and composition it is used in the semiconductor fabrication furnaces.

Fused quartz has nearly ideal properties for fabricating first surface mirrors such as those used in telescopes. The material behaves in a predictable way and allows the optical fabricator to put a very smooth polish onto the surface and produce the desired figure with fewer testing iterations. In some instances, fused quartz has been used to make the individual elements of special purpose lens, such as the Zeiss 105mm f/4.3 UV Sonnar lens for the Hasselblad camera. This lens is used for UV photography, as the quartz has a lower extinction rate than lens made with more common flint or crown formulas.

Fused silica as an industrial raw material is used to make various refractory shapes such as crucibles, trays, shrouds, and rollers for many high temperature thermal processes including steelmaking, investment casting, and glass manufacture. Refractory shapes made from fused silica have excellent thermal shock resistance and are chemically inert to most elements and compounds including virtually all acids, regardless of concentration, except hydrofluoric acid which is very reactive even in fairly low concentrations. Translucent fused silica tubes are commonly used to sheathe electric elements in room heaters, industrial furnaces and other similar applications.

Physical properties

The extremely low coefficient of thermal expansion, about 0.55 ppm/°C (20-320°C), accounts for its remarkable ability to undergo large, rapid temperature changes without cracking (see thermal shock).

Fused quartz is prone to phosphorescence and "solarization" (purplish discoloration) under intense UV illumination, as is often seen in flashtubes.^[1]

"UV grade" synthetic fused silica (sold under various tradenames including "HPFS", "Spectrosil" and "Suprasil") has a very low metallic impurity content making it transparent deeper into the ultraviolet. An optic with a thickness of 1 cm will have a transmittance of about 50% at a wavelength of 170 nm, which drops to only a few percent at 160 nm. However, its infrared transmission is limited by strong water absorptions at 2.2 μm and 2.7 μm.

"IR grade" fused quartz (tradenames "Infrasil", "Vitreosil IR" and others) which is electrically fused, has a greater presence of metallic impurities, limiting its UV transmittance wavelength to around 250 nm, but a much lower water content, leading to excellent infrared transmission up to 3.6 μm wavelength. All grades of transparent fused quartz/fused silica have near-identical physical properties.

The water content (and therefore infrared transmission of fused quartz and fused silica) is determined by the manufacturing process. Flame fused material always has a higher water content due to the combination of the hydrocarbons and oxygen fuelling the furnace forming hydroxyl [OH] within the material. An IR grade material typically has an [OH] content of <10 parts per million.

Optical properties

Dispersion of fused silica can be approximated by the following Sellmeier equation (Malitson 1965):

$$\varepsilon = n^2 = 1 + \frac{a_1 \lambda^2}{\lambda^2 - l_1^2} + \frac{a_2 \lambda^2}{\lambda^2 - l_2^2} + \frac{a_3 \lambda^2}{\lambda^2 - l_3^2},$$

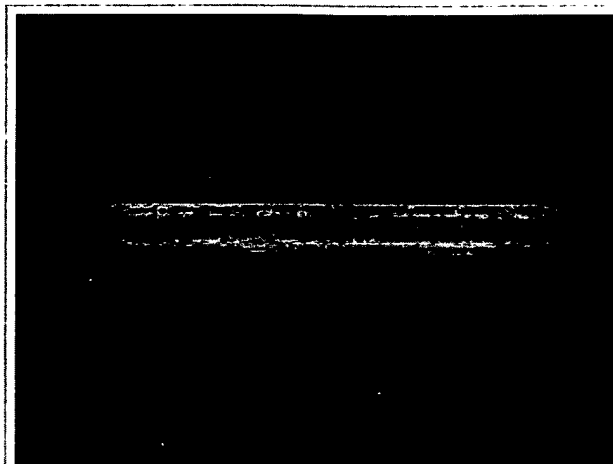
where

$$\begin{aligned} a_1 &= 0.69616630, & l_1 &= 0.068404300, \\ a_2 &= 0.40794260, & l_2 &= 0.11624140, \\ a_3 &= 0.89747940, & l_3 &= 9.8961610, \end{aligned}$$

and wavelength is measured in micrometers.

This equation is valid between 0.21 micrometres and 3.71 micrometres (see ref).

Change of Refractive Index with Temperature (0° to 700°C): $1.28 \times 10^{-5}/^{\circ}\text{C}$



Phosphorescence in fused quartz from an extremely intense pulse of ultraviolet light, centered at 170 nm, in a flashtube.

Typical properties of clear fused silica

- Density: 2.203 g/cm³
- Hardness: 5.3–6.5 (Mohs Scale) , 8.8 GPa
- Tensile strength: 48.3 MPa
- Compressive strength: >1.1 GPa
- Bulk modulus: ~37 GPa
- Rigidity modulus: 31 GPa
- Young's modulus: 71.7 GPa
- Poisson's ratio: 0.16
- Lamé elastic constants: $\lambda=15.872$ GPa, $\mu=31.261$ GPa
- Coefficient of thermal expansion: $5.5\times 10^{-7}/^{\circ}\text{C}$ (average from 20 °C to 320 °C)
- Thermal conductivity: 1.3 W/(m·K)
- Specific heat capacity: 45.3 J/(mol·K)
- Softening point: c. 1665 °C
- Annealing point: c. 1140 °C
- Strain point: 1070 °C
- Electrical resistivity: $>10^{18}$ Ω·m
- Dielectric constant: 3.75 at 20 °C 1 MHz
- Dielectric loss factor: less than 0.0004 at 20 °C 1 MHz
- Index of refraction: at 587.6 nm (n_d): 1.4585
- Strain-optic coefficients: $p_{11}=0.113$, $p_{12}=0.252$.
- Hamaker Constant: $A=6.5$ zJ.
- Dielectric strength: 4.7-6.7 MV/cm

See also

- Quartz
- Silica (fused silica hardness = 8-10 GPa)
- Vycor
- Aqua aura
- Glass
- List of minerals

External links

- Momentive (<http://www.momentivequartz.com/>) World leader in the manufacturing of clear and translucent tubing; rods and solid shapes; and fused crucibles for growing single crystal silicon.
- [1] (<http://www.technicalglass.com/>) Fabricator and Supplier of Fused Quartz Products
- Saint-Gobain Quartz (<http://www.quartz.saint-gobain.com/>) Manufacturer of fused quartz and fused silica materials and products with downloadable data sheets in the Library
- Fused silica (<http://www.newrise-llc.com/fused-silica.html>) contains a list of commercially available fused silica glasses
- Translume (<http://www.translume.com/>) Micromachining contractor in USA that works exclusively with fused silica glass.
- Heraeus Quarzglas (http://www.heraeus-quarzglas.de/en/quarzglas/quarzglas_1/Quarzglas.aspx) Detailed information about properties, chemical behavior, nomenclature etc.

- [2] (<http://www.gmassoc.com/>) Expert Quartz Machining and Fabrication worldwide

References

1. ^ http://optoelectronics.perkinelmer.com/content/RelatedLinks/CAT_flash.pdf

- Malitson, I.H. "Interspecimen Comparison of the Refractive Index of Fused Silica," (<http://adsabs.harvard.edu/abs/1965JOSA...55.1205M>) Journal of the Optical Society of America 55, no. 10 (October 1965): 1205-1209. DOI:10.1364/JOSA.55.001205 (<http://dx.doi.org/10.1364/JOSA.55.001205>).

Retrieved from "http://en.wikipedia.org/wiki/Fused_quartz"

Categories: [Chemical engineering](#) | [Glass compositions](#) | [Transparent materials](#) | [Silicon compounds](#)

- This page was last modified on 6 October 2009 at 18:09.
- Text is available under the Creative Commons Attribution-ShareAlike License; additional terms may apply. See Terms of Use for details.
Wikipedia® is a registered trademark of the Wikimedia Foundation, Inc., a non-profit organization.

PROPERTIES AND STRUCTURE OF VITREOUS SILICA. I

R. BRÖCKNER

Max-Planck Institut für Silikatforschung, Würzburg, Germany

Received 29 January 1970

This review is concerned with the properties and structure of silica glass. The following topics are treated:

Types of silica glasses;

The vitreous state of silica glasses: thermodynamical approach, atomistic approach;

Optical properties: absorption and fluorescence, refractive index and homogeneity;

Mechanical and thermal properties: specific volume, volume relaxation, volume and pressure, elastic and internal friction behaviour, heat capacity and heat conduction, strength, crystallization.

Introduction

The ability of silica to form a series of, not less than 22 modifications¹⁾ (not all are modifications in the strong crystallographic sense) from the nearly perfect crystalline quartz to the highly disordered amorphous silica-M, an amorphous phase formed by the action of high speed neutrons, and to the silica glass, is responsible for the great interest in the chemically simple substance SiO_2 . Furthermore three main reasons are responsible for another great practical and theoretical interest in SiO_2 , especially in that of silica glass: a) the excellent physical (mechanical, thermal and optical) properties simultaneously connected with excellent chemical resistance, b) the characteristic anomalies of silica glass in comparison to other glasses of mixed type, among these also is the group of silicate glasses, and other glass formers, and c) last but not least, is the significance of SiO_2 as the chief component of the wide variety class of silicate glasses.

It is beyond the scope of this article to present a complete stand of knowledge of the head-line topic, because this would demand a book-like scale. But it will be tried under this restriction to give a review with considerations and aspects on more recent developments in the termed field with befitting regard to the respectable precedent investigations.

1. Types of silica glasses

The increasing and different demands in the properties of silica glasses in

the last two decades required increasing effort in melting processes of silica. This development has not come to an end yet but is still in vigorous progress. To day we have to distinguish between different kinds of silica glasses with respect to properties and structure, there are about four types commercially available²⁾:

Type I - silica glasses are produced from natural quartz by electrical fusion under vacuum or under an inert gas atmosphere. They contain nearly no OH-groups (about 5 ppm or less) but relatively high metallic impurities of the order of 30-100 ppm Al and 4 ppm Na (all in weight fractions). Commercial names are Infrasil³⁾, IR-Vitreosil⁴⁾, G. E. 105, 201, 204⁵⁾.

Type II - silica glasses are produced from quartz crystal powder by flame fusion (Verneille-process). Because of the partial volatilization and the absence of any crucible material the metallic impurities are less than in type I silica glasses, but the atmosphere of the hydrogen-oxygen flame causes an OH-content of about 150-400 ppm. Trade names are Herasil, Homosil, Optosil³⁾, O.G. Vitreosil⁴⁾, G.E. 104⁵⁾. A special thermal treatment in oxygen atmosphere, causing a good optical transparency in the ultraviolet range, leads to Ultrasil³⁾ silica glass.

Type III - silica glasses are synthetic vitreous silicas produced by hydrolyzation of SiCl_4 when spraying into an oxygen-hydrogen flame. This material is practically free from metallic impurities, but contains a high amount of OH, in the order of 1000 ppm, and because of the starting material Cl in quantities of the order of 100 ppm. Trade names: Suprasil³⁾, Spectrosil⁴⁾, Corning 7940⁶⁾.

Type IV - silica glasses are also synthetic vitreous silicas produced from SiCl_4 in a water vapour-free plasma flame. These silica glasses are similar to type III but contain only about 0.4 ppm OH and about 200 ppm Cl. Trade names: Suprasil W³⁾, Spectrosil WF⁴⁾, Corning 7943⁶⁾. Another type was produced but only in a single case and on a laboratory scale⁷⁾. The starting material was silicon of semiconductor-quality which was oxidized in pure oxygen high-frequency plasma flame. The impurity content, especially the OH-content, was extremely low.

The different types of silica glasses have different selective properties and therefore characteristic differences in their network fine structure. This fact and especially the numerous anomalous properties of silica glass at all will be considered in the following sections.

2. The vitreous state of silica glasses

2.1. THERMODYNAMICAL APPROACH

Silica has the ability to form a supercooled liquid by cooling down from

temperatures above the melting point of the high temperature modification of cristobalite and to freeze-in to a solid glass. In spite of the fact that the silicate glasses owe their ability of glass-forming mostly to the silica content, the properties of the silica glass itself differ widely from those of the silicate glasses, although silica is the chief component of all silicate glasses.

If one considers the typical behaviour of a common silicate glass as a function of temperature, it is evident, that for a glass-forming substance on cooling down the melt will undercool, freeze-in⁹⁾ and change to a glass measurable by a discontinuity in form of a crack of any thermodynamical property, the enthalpy H , the free energy F , or the volume V respectively, or in a break of the first differential quotient. This crack is neither a transformation point of a first nor such of a second order in the sense of Ehrenfest⁸⁾, but a transition, in the English terminology: a glass transition "point", t_g . The characteristic difference between such a point and a second-order transformation point t_2 is given by the kinetic behaviour of these points. When a substance with a second-order transition point is quenched from high temperatures, that point will be shifted to lower temperatures in comparison to a slower cooling rate.

On the other hand the glass transition point will be shifted to higher temperatures by those two treatments (fig. 1). This is the typical behaviour which differentiates the group of glasses from other materials, especially from crystalline and possibly from most other amorphous materials⁹⁾ *.

In the case of silica glass we have to consider a first anomalous behaviour¹¹⁾. The volume-temperature curve shows a minimum at a temperature of about 1500°C in the structural (metastable) equilibrium of the (undercooled) melt¹²⁾ and also a minimum at about -80°C in the glassy state. The volume behaviour on quenching in the high-temperature branch of the equilibrium curve (above 1500°C, see fig. 2) is the same as in the case of the common silicate glasses (fig. 1) but not measurable (because of crystallization and of too short relaxation times). In the anomalous region (1000-1500°C) the behaviour is different, especially if one considers the volume behaviour on reheating of a quenched sample (arrows in fig. 2). The volume shifts in the direction of the equilibrium curve are contrary to those of common silicate and other glasses (compare fig. 1): but the qualitatively similar behaviour is the direction of the temperature-shift of the glass transition "point" on quenching to higher temperatures with increasing quenching rate. Therefore vitreous silica is "really a glass".

For experimental determination, when the metastable structural equi-

* It was tried theoretically to correlate these two points t_2 and t_g , and pointed out in ref. 10 that under the special case of very low cooling rates t_g may be considered as a t_2 -point and treated as that to a certain degree.

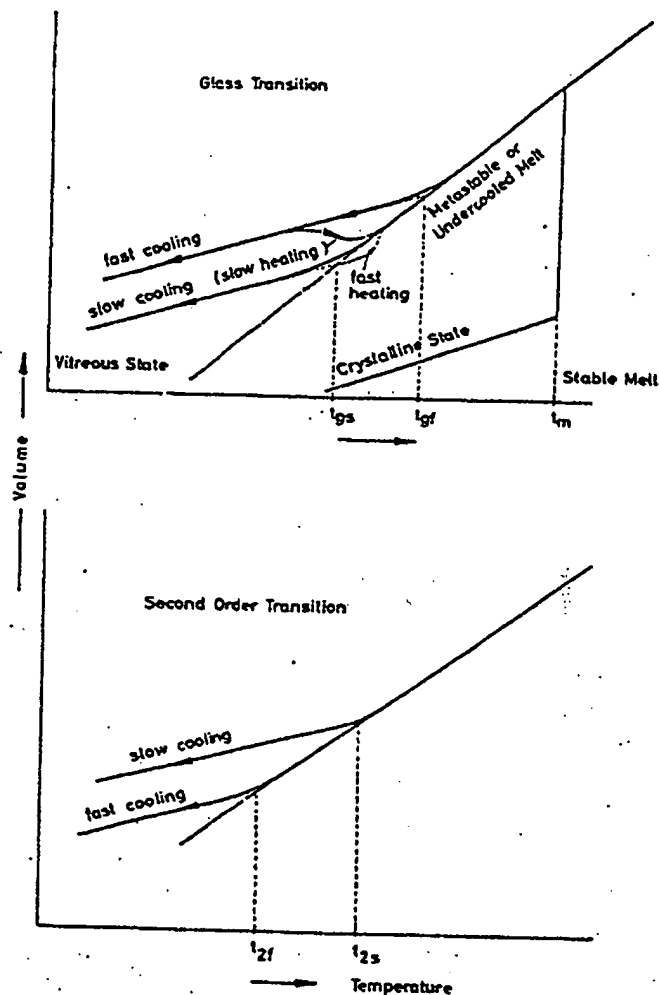


Fig. 1. Schematic diagram of volume-temperature plot for common glasses under various cooling rates in comparison to substances with a second-order transition. Here, t_g = glass transition temperature; t_2 = second order transformation temperature; f = fast, s = slow cooling rate; t_m = melting or liquidus temperature.

Equilibrium curve of any substance expected to be a glass is not so easily available as in the case of typical glasses (because crystallization or decomposition might occur at temperatures above t_g), the following method may be applied. The quenched sample is held at a constant temperature below the presumable t_g at which the volume relaxation times are experimentally desirable and at which the sample is not altered by crystalli-

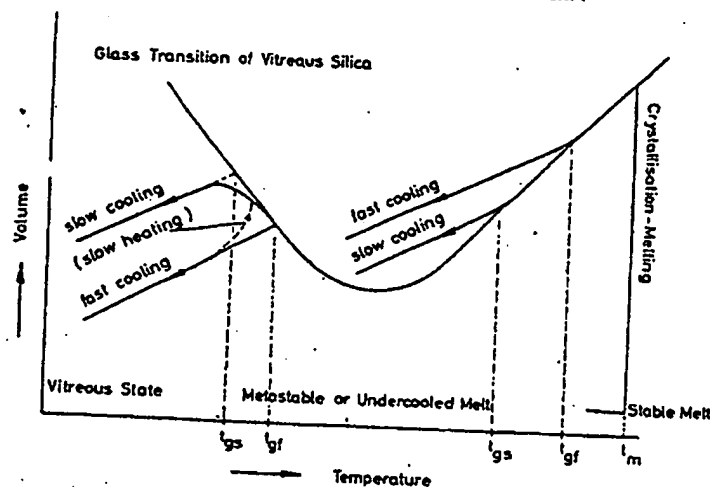


Fig. 2. Schematic diagram of volume-temperature plot for vitreous silica (types I and II). On the abscissa, t_{gs} means glass transition temperature for slow and t_{gf} for fast cooling. On the left side of the minimum, the cooling time may range from seconds ("fast" cooling) up to days ("slow" cooling), however, on the right side, they may be of the order of milliseconds (or shorter) for "fast" cooling, and one tenth of a second for "slow" cooling.

zation or decomposition, and the volume change is observed after different quenching rates. This procedure is repeated at several, or at least at two, temperatures. Two informations are obtained from those experiments: the sign and possibly also the amount of the slope of the metastable equilibrium curve and the shift of t_g with increasing quenching rate of the sample, and therefore the decision whether the material in question is a real glass or not.

2.2. ATOMISTIC APPROACH

As known from X-ray¹³⁻²⁰ and neutron diffraction^{21,22} of silica glass the structural unit consists, like that of most crystalline modifications of silica, of four oxygen atoms placed at the corners of a tetrahedron with a silicon atom at the center. This statement is well accepted by all authors, as well as the distances between Si-O (1.58 Å), O-O (2.6 Å), and Si-Si (3.2 Å) but not the arrangement of the tetrahedrons forming the cooperative structure.

The geometrical structure concept of oxide glasses at all are very closely related to those of the silica glass structure and may be divided into four groups.

Group I is due to the concept of the random network hypothesis originally stated by Zachariasen²³, X-ray proofed by Warren et al.¹³⁻¹⁵, confirmed

and modified by a series of authors as Dietzel²⁴), Stevels²⁵⁻²⁷), Sun²⁸) and Huggins²⁹).

Group II is based on the concept of the crystallite hypothesis by Lebedev³⁰), X-ray examined by Randall, Rooksby et al.¹⁸), Hartleif¹⁹) and modified by Porai-Koshits²⁰) and Botvinkin³¹).

Group III is based on the microheterogeneous structure concept first claimed by Dietzel^{24, 51}) as "latent decomposition" in systems with an S-shaped liquidus curve, put forward by Vogel³²⁻³⁴) and brought to a thermodynamic-statistical base of phase separation, nucleation and decomposition by Cahn^{35, 36, 38}), Hillig³⁷), Turnbull^{39, 40}) and Charles⁴¹).

Group IV includes all those hypotheses which are based either on a special a priori-model as that of Tilton's⁴²) vitron model (pentagonal dodecahedra), Robinson's⁴³) rod-like model and so on, or based on pure statistical models of certain partition functions as put forward by Bell, Dean et al.^{44, 45}).

Besides these geometrical pictures of glass structure, the more energetic structural concepts of oxide glasses are to be distinguished; they may be divided into two other groups.

Group V is characterized by the mixed binding concept of Smekal^{46, 47}). In oxide glasses the mixed binding forces are of covalent and heterovalent character and in silica glass this mixture is about 50:50%. Similar statements were made by Grjotheim and Krogh-Moe⁴⁸) who postulated electronegativities around 2 ± 0.2 eV as a supposition for glass forming. Winter⁴⁹) suggested that the p-electrons should be responsible for glass forming. In addition to Smekal's concept a third kind of binding force is discussed by Noll⁵⁰), the double bonding between Si and O, so that three mixed binding forces, with almost equal proportions, are acting in silica.

Group VI is due to the concept of the field strength after Dietzel^{24, 51}), based on the simple electrostatic Coulomb attraction force and due to the concept of the screening theory after Weyl^{52, 53}). In both concepts the important factor is the polarization of anions and cations, which, as a first approximation, might be regarded as the covalent part of the mixed binding force concept.

To day, glass scientists tend to regard the groups I and II as ideal types or as limit models of possible glass structures and in this sense they are very helpful for the understanding of special kinds of behaviour of glasses. A better approach to the real glass structure gives group III when groups I and II are included, while group IV starts from a more formalistic point of view. All these geometrical concepts give no answer to the question: why is a substance able to go into the vitreous state? Interpretations were tried on account of the more or less polymeric overall network, that the undercooled

melt of substances of that kind has a high viscosity in the neighbourhood of the glass transition range and therefore nucleation and crystallization rates are very low. That means, that the glass forming process is a kinetic problem and therefore depends in principle only on the rate of quenching. But this is not a true interpretation, because it only shifts the problem from one property to another one.

In the author's opinion the energetic structural concepts are going back to deeper origins. While the field strength concept is concerned with the binding forces between cations and anions, the screening theory⁵³⁾, and also former considerations on the coordination tendency⁵¹⁾, consider the relations in and between the polyeders, and factors are to be regarded as the polarization, the coordination number and, in the case of multi-component glasses, the ratio of network forming to network modifying cations, trying to regard the whole cooperative problem of the structure of glasses.

Possibly a further step forward in the future will be made in a more definite way than was done by Smekal's mixed binding hypothesis (many non-glass-forming substances have also mixed binding forces) by the application of the hybrid-function concept, which was successfully applied to amorphous semiconductor materials and non-oxide glasses (chalcogenide glasses) by Krebs⁵⁴⁾. While the former concept only claims a mixed bonding in general, the hybrid-function concept may give a more specified selection of glass-forming substances because one may get information on the directions of the covalent part of the binding forces and possibly on their distribution around the building units.

3. Optical properties

3.1. ABSORPTION AND FLUORESCENCE

The optical absorption behaviour of silica glasses is determined by impurities and defects in the structural arrangement in addition to transitions of the electrons of the bridging oxygens into the conduction band (uv-edge) and of the Si-O atomic resonance vibrations (infrared bands).

a) The ultraviolet-edge limits the transmission of an electromagnetic wave to the high frequency side by the interaction with the electrons of a material. This interaction will occur at higher frequencies for stronger bonded electrons. That means not only in the case of glasses will the uv-edge be shifted to shorter wavelengths, but this will also occur where higher binding strengths between the atoms and cations and a smaller amount of weak crystalline or amorphous network defects are. Therefore the most "perfect" silica glasses, regarded as especially "pure", like the type III and IV silica glasses, have the best transmittance properties [(fig. 3. see also b), next page].

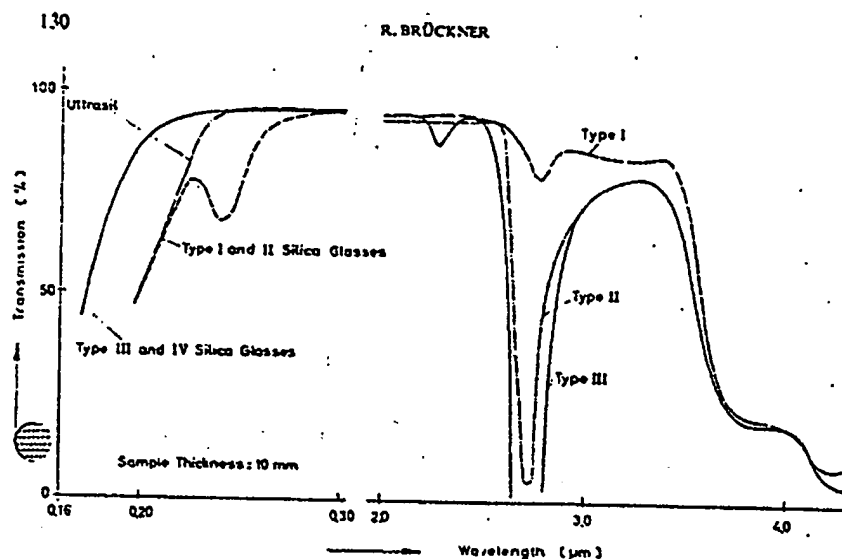


Fig. 3. Transmission curves as a function of wavelength⁷³.

b) The effect of *impurities and network imperfections* on the absorption of light is due to the energy loss produced by the so-called colour centers consisting of electrons and defect electrons, possibly forming a paramagnetic centre. Those centres give rise to absorption at definite frequencies of electromagnetic waves.

The absorption band near $0.240 \mu\text{m}$ (fig. 3) observed in type I and II silica glasses only, corresponds to the fluorescence radiation at 0.280 and $0.390 \mu\text{m}$. Its origin is not yet totally clear but it may be contributed to both reduction and impurities, above all germanium and aluminium⁵⁵⁻⁵⁸. Partial reduction of SiO_2 to SiO_{2-x} , where x is of the order of 10^{-4-5} (ref. 56), especially at locations of impurity atoms, causes a weakening of the network bonding which means that the electrons at these centres are pushed into the conduction band and have lower energies than those of the network and therefore absorb lower energy of light.

Type III and IV silica glasses do not show the $0.240 \mu\text{m}$ absorption and the corresponding fluorescence radiation because they contain nearly no impurities, except hydroxyl groups. But the binding force of the proton is so strong that the energy of the electrons at the SiOH -centres will not be reduced in comparison to those of the perfect SiO_2 -network. This is independent of the fact, that OH-groups weaken the glass network as a whole considerably (see sections 4.4. and 5.4.)

When silica glasses of type I and II are irradiated by X-rays, γ -rays or

neutrons they become as brown as smoky quartz and show three absorption bands near 0.220, 0.300 and 0.550 μm ; these bands are stronger for type I than for type II at comparable doses^{59,60}). This is due to colour centres with adequate lower energy states of the corresponding electrons. These energy states depend on the type of the network imperfections especially caused by Al-centres damaged in different manners for which Stevels⁶¹) gives special structural plausible interpretations, according to which the removal of an oxygen from the AlO_4 -complex leaves behind a vacancy (0.550 μm band) or is excited by radiation processes into an existing vacancy of a double Al-centre (0.300 μm band). It is possible to heal the defect centres by heating the glass to moderate temperatures ($\sim 400^\circ\text{C}$); meanwhile definite luminescence glow curves are observed at 160, 215 (weak) 380 and 590 $^\circ\text{K}$ ⁶²⁻⁶⁴).

In irradiated silica glasses of type III and IV no visible colour effects occur, but only the 0.220 μm absorption band is slightly shifted to 0.215 μm . The origin of this absorption is not clear, a certain connection with OH-groups is believed to be evident^{59,60}) by optical and ESR-measurements. Possibly it is due to an electron transition of a non-bridging oxygen into the conduction band. The corresponding electron transition of a bridging oxygen is due to an absorption below 0.180 μm .

c) Going to longer wave lengths one observes the next absorption at 2.78 μm with higher combination vibrations or overtones at 2.4 and 2.2 μm , produced by the *oscillations of the OH-group*. As in other oxide glass formers (B_2O_3 , GeO_2), only the free OH-group exists in silica glasses, contrary to the mixed silicate glasses in which also bonded OH-groups with more or less strong hydrogen bridges to other non-bridging oxygens exist corresponding to 3.6 and 4.2 μm absorption bands respectively^{65,66}).

d) The *Si-O oscillations* produce absorptions at 9.0, 12.5 and 21 μm in the infrared and at 12.5 μm in the Raman-spectrum in the form of broad bands in comparison to quartz and cristobalite. The broadening effect is usual for all glasses and is the result of the amorphous structure giving rise to a broader distribution of the possible oscillations than in the ordered arrangements of the corresponding crystalline modifications. The 9.0 μm band is associated with the antisymmetrical Si-O valency vibration ($\leftarrow\text{Si}-\text{O}\rightarrow\leftarrow\text{Si}$), the 21 μm band with the bending vibration of Si-O-Si and O-Si-O respectively, and the 12.5 μm band with the symmetrical Si-O valency vibration ($\leftarrow\text{Si}-\text{O}-\text{Si}\rightarrow$) which should be infrared inactive and which is the strongest Raman-line⁶⁷⁻⁶⁹). Possibly anisometrical influences resulting from cooperative network deformations give rise to an antisymmetrical component of the symmetric pumping vibration at 12.5 μm with an electric dipole moment.

With reference to thermal history, there was observed a slight but measurable shift of the 12.5 μm band in transmitting light to shorter wave lengths

with increasing density⁷⁰) as a function of fictive temperature (see section 4.1.); no shift of the other two bands was observed. On the other hand, also a shift of the 9.0 and 21 μm band, but to longer wave lengths, was observed in reflecting light⁷¹).

A calculation of the force constants⁶⁸) leads to a value of $K_{\text{Si-O}} = 4.0 \times 10^5$ dyne/cm, which is higher in comparison to the GeO_2 and BeF_2 -glasses by a factor of 1.2 and 3.6 respectively being in good agreement with calculated relative Coulombic binding forces.

3.2. REFRACTIVE INDEX AND HOMOGENEITY

The refractive index is shown in fig. 4⁷²) as a function of wavelength, from which the dispersion function may be obtained by differentiation. There is a very slight difference (in the order of about 0.0002) between the

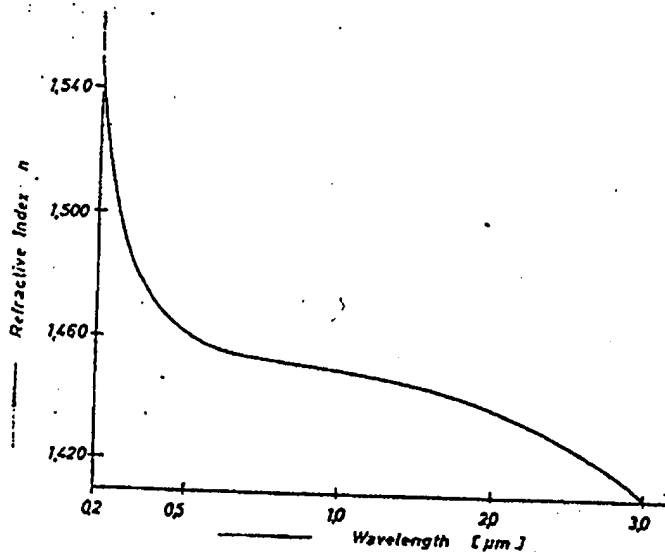


Fig. 4. Refractive index as a function of wavelength⁷²).

refractive index [and density⁷³] of type III and type II silica glasses, the index of the natural silica glasses being the higher one. It is obvious that this difference is due to the water content, according to ref. 73, in contrast to mixed silicate glasses⁷⁴) and to B_2O_3 glass^{75,76}). This behaviour may be interpreted as follows: in silica glass only the free OH-group, without hydrogen bonding, is existent, whereas in mixed silicate glasses the existence of hydrogen bonding causes shrinkage in the glass network, which results in

133

* That the B_2O_3 -glass shows an increase of n with increasing water content although only free OH-groups are present as in the case of silica, is interpreted by local network contractions in the neighbourhood of free OH-groups caused by the lower valency and the flat arrangement of the BO_3 -group; if a B-O-bond is "broken" by one proton and an OH-group, the connection of B to the network is only two-fold leading to a closer contact of a BOH-group to the network and to a general contraction ⁷⁷).

and 35°C. But for changes of optical lengths in optical arrangements not only dn/dT but also $\partial n/\partial T$ is of importance.

In fig. 5 the total temperature dependence of n is given for a type II silica glass. The discontinuities at 250 and 500°C are regarded as a result of crystalline structural units⁷³).

As a function of thermal history, the refractive index shows a maximum as in the case of the density (see section 4.1.) at a fictive temperature of about 1500°C (fig. 6)⁷⁵). The values are measured from water-quenched samples which were brought into structural equilibrium at the corresponding fictive temperature. Structural equilibrium means that no changes in n take place with time at constant fictive temperature. The scattering of measurements mainly arises from the birefringence of the quenched samples, caused by thermal stresses. This effect and also the discontinuities of $n=n(T)$ are discussed later in connection with volume and diffusion.

Two kinds of optical inhomogeneities are observed in silica glasses: steady changes of the refractive index and the so-called grain structure. To day, qualities are produced with long range inhomogeneities of the order of

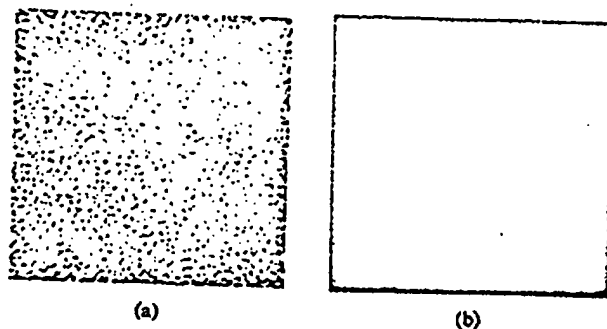


Fig. 7. Pin-hole pictures of Herasil (a) and Homosil silica glass (b)⁷²

$\Delta n = 2.5 \times 10^{-6}$ or better^{79,80}). Silica glasses which are not carefully homogenized (second and third class quality) show a grain structure (fig. 7) when observed with the pin hole method⁷²). This grain structure obviously is the result of an incomplete melting process.

4. Mechanical and thermal properties

4.1. SPECIFIC VOLUME

The principal volume-temperature behaviour was already described in section 2.1., fig. 2, but it should be shown in more detail with respect to two

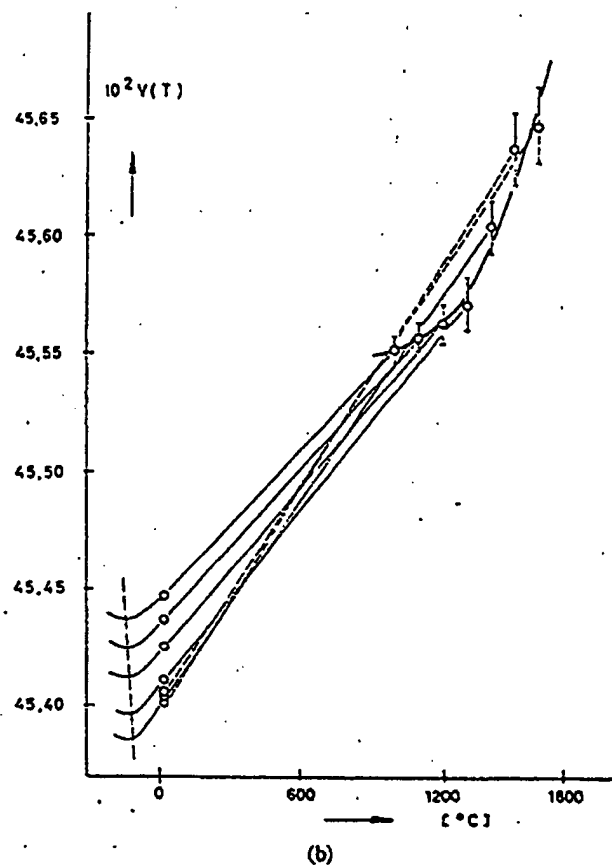
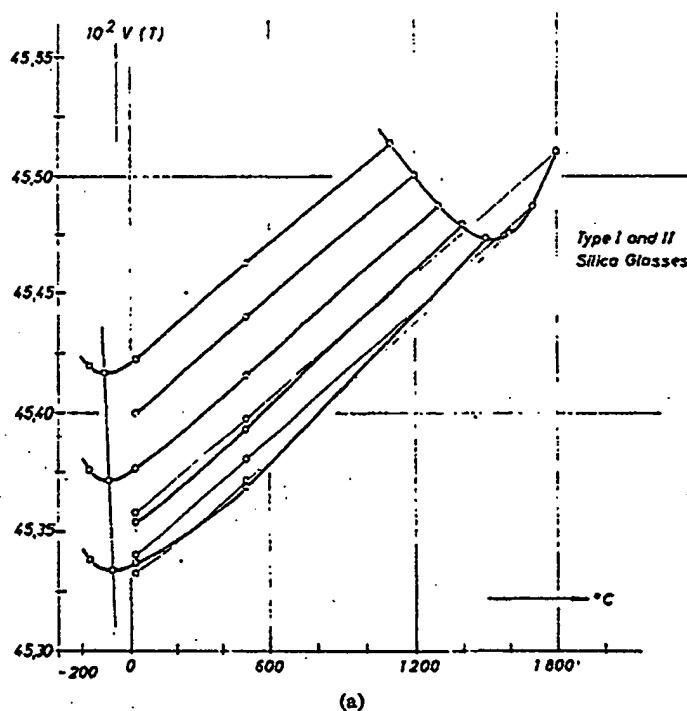


Fig. 8. Volume-temperature plot for type I/II (a) and for type III silica glasses (b) respectively.

pure than the type I/II silica glasses. Therefore, the behaviour of the "water"-rich silica glasses in fig. 8b may be regarded as a first step from the "classical" type I/II silica glasses in the direction of the common multi-component silicate glasses.

The volume-temperature behaviour in the metastable region of the silica melt is completed in fig. 10 by density measurements⁸¹⁾ in the stable melt at temperatures above the melting point of cristobalite. As it is seen from this figure the high temperature branch has a steeper slope than that found from the measurements in the metastable range below 1720°C. The reason of this is, that at temperatures of about 1600°C and above the volume relaxation times

groups of silica glasses, the type I and II (natural) and type III (synthetic silica glasses) respectively (figs. 8 and 9)^{70, 75}. Both groups differ distinctly and are well measurable in density at room temperature; both groups show the characteristic maximum corresponding to a fictive temperature of 1550°C (type I/II glasses) and 1460°C (type III glasses) respectively. But if one calculates the specific volume for the metastable equilibrium fictive temperatures with the help of thermal expansion measurements (see fig. 12), two qualitatively and quantitatively different structural equilibrium curves are obtained (figs. 8a and 8b). While the type I/II silica glasses show a minimum volume at 1550°C, the type III silica glasses do not show this; the "anomalous" volume branch from 1000 to 1500°C is turned to a more "normal" branch with a very low positive volume-temperature coefficient. This coefficient is so small with respect to that of the glass, that at room temperature still an "anomalous" volume behaviour results (fig. 9). The high-temperature volume behaviour (fig. 8) is easy to understand if the action of the high OH-content of the type III glasses is similar to that of the alkali oxides, because if one regards the OH-content as impurity, the type III glasses are more im-



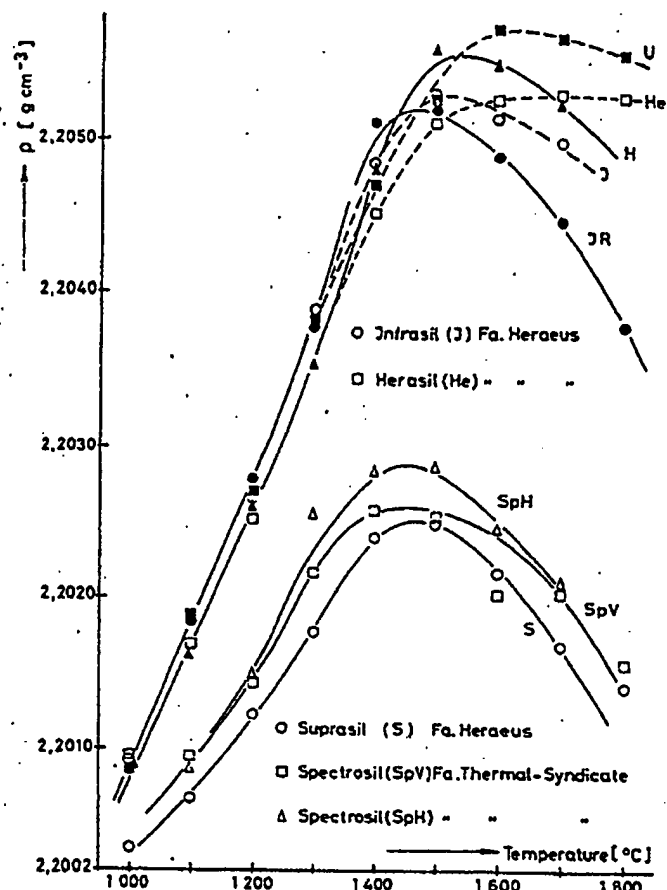


Fig. 9. Density, of different silica glasses of type I/II and III, as a function of fictive temperature. ● Vitreosil (JR) Fa. Thermal-Syndicate; ▲ Homosil (H) Fa. Heraeus; ■ Ultrasil (U) Fa. Heraeus.

become smaller than the quenching time of the samples* [concerning the method of these measurements in the metastable range it is referred to the original literature⁷⁵].

The volume-temperature behaviour in the glassy state is shown in fig. 11

* Within the scope of this review it only may be said that the metastable equilibrium curve of fig. 8 is obtained by keeping the (thin) samples as long, at constant temperatures, as a constant density is measured at room temperature after quenching into water. Corrections of the room temperature values to the fictive temperature were carried out by thermal expansion measurements (see below) of samples with the same thermal history (fictive temperatures).

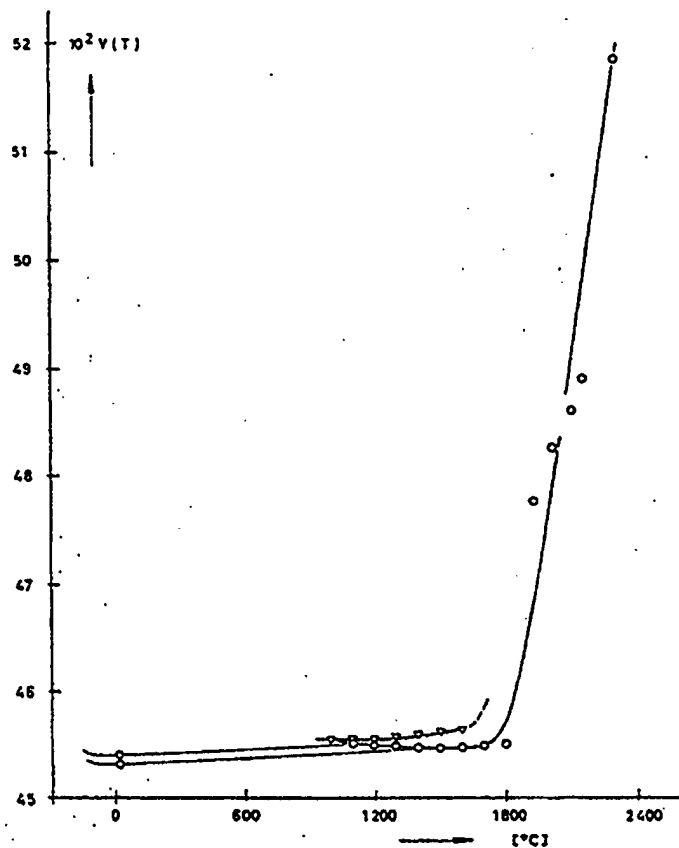


Fig. 10. Volume-temperature diagram including measurements¹¹⁾ at temperatures above the melting point of cristobalite. O type I/II; V type III silica glasses.

in the form of thermal expansion curves of type II silica glass samples of different fictive temperatures. Those samples with a fictive temperature corresponding to the minimum of the specific volume at 1550°C or 1460°C respectively have the highest thermal expansion, those of higher or lower fictive temperatures have a lower thermal expansion (fig. 12). This is in agreement with the Grüneisen relation:

$$\beta c_v / \alpha V = \text{constant},$$

where β = compressibility, c_v = specific heat, α = expansion coefficient and V = specific volume.

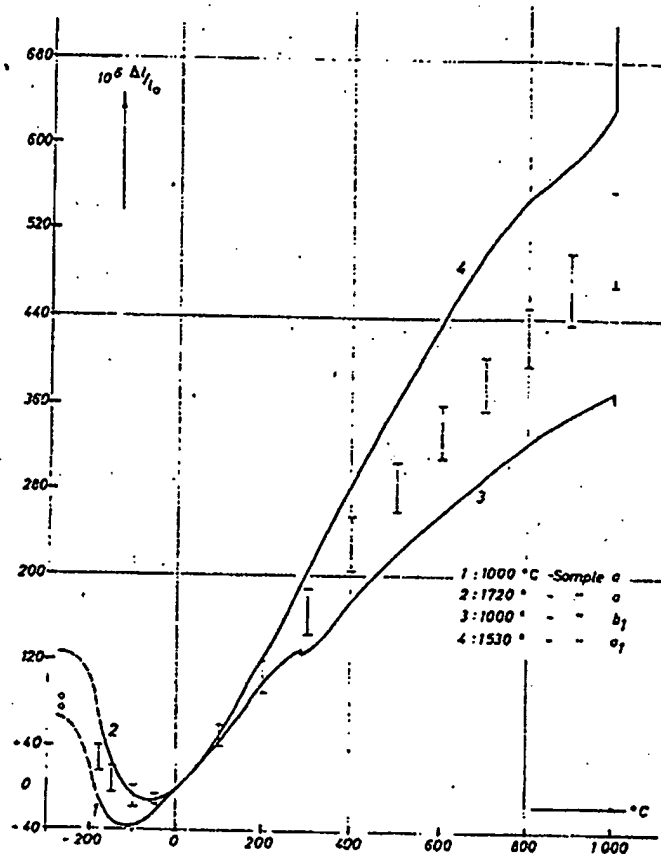


Fig. 11. Thermal expansion of silica glasses (type I/II) of different fictive temperatures. Vertical bars: range of older literature data; O: values at 5°K after Keesom and Doborzynski²⁷.

In the low temperature range, below room temperature, another relation between fictive temperature and volume exists. A characteristic point is the low temperature minimum of the volume. It is shifted to higher temperatures with increasing fictive temperature, regardless of the high temperature volume minimum. There is a linear relationship between minimum temperature and fictive temperature within the limit of error (fig. 13). Again a difference between the group of natural and synthetic silica glasses is found. According to a lower high temperature minimum of the synthetic silica

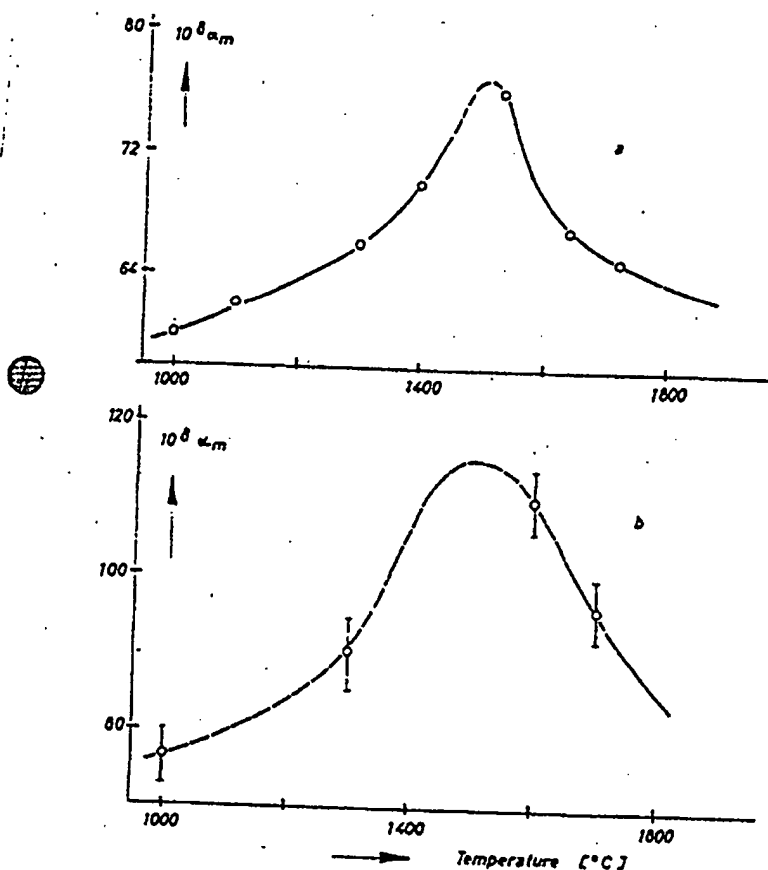


Fig. 12. Thermal expansion coefficient of type I/II (a), and III (b), silica glasses as a function of fictive temperature.

glasses, a lower low temperature minimum is found in comparison to the natural silica glasses.

The effect of low temperature negative thermal expansion of vitreous silica, as well as that of high-cristobalite and high-quartz, may be understood qualitatively with special regard to the transverse vibrations of the oxygen atoms and with the concept that the major contribution to the thermal behaviour is from transverse oxygen vibrations⁸³, due to the openness of structure and the great freedom of transverse vibrations. It should be expected that most frequencies of the vibrations in an ionic crystal increase when the structure shrinks, because the ions have to move against the strong

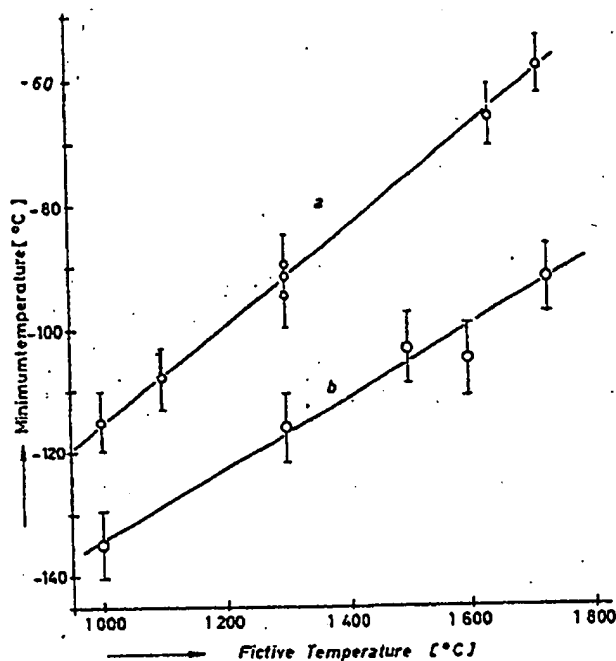


Fig. 13. Minimum temperature (range -135 to -60°C) as a function of fictive temperature: (a) type I/II, (b) type III silica glasses.

repulsive forces of the approaching neighbours. If the structure permits one or more of the natural frequencies to decrease as the structure shrinks, there will be a possibility for negative expansion, and this seems to be the case for vitreous silica among other substances (Si, Zn S, and InSb), being not only connected to the vitreous state.

4.2. VOLUME RELAXATIONS

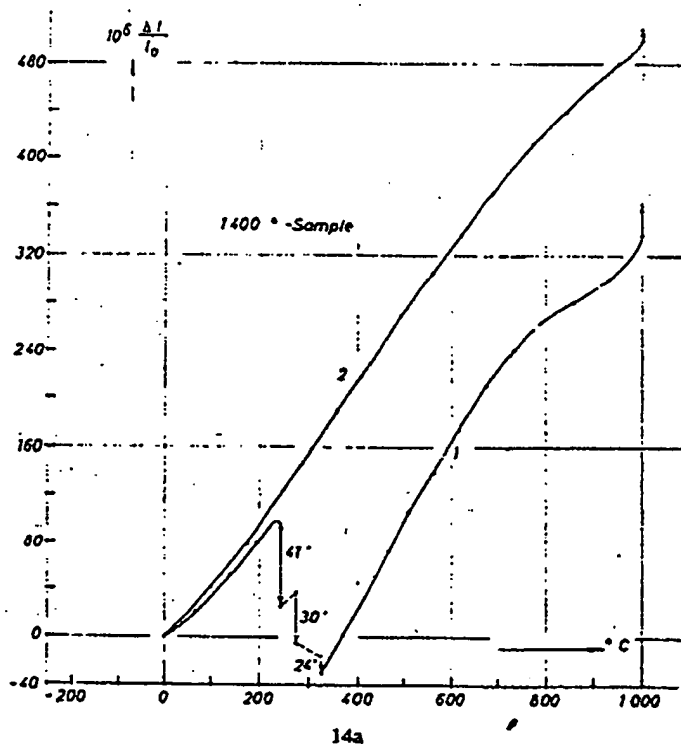
Three kinds of volume relaxation can be observed during the measurement of thermal expansion of heat-treated and quenched silica glass samples (fig. 14)^{70,75}.

a) At 1000°C the influence of the glass transition is perceivable, the sample tends to the metastable equilibrium curve as already shown in principle in fig. 1; in the example of fig. 14a a sample with a fictive temperature of 1400°C shows the same effect. The relaxation time at 1000°C is of the order of few hours, depending on the fictive temperature and accordingly on the "distance" from the metastable equilibrium curve. It is estimated that the

glass transition temperature is about 1100°C for the group of natural silica glasses.

The group of artificial silica glasses has a lower glass transition temperature at about 1000°C. This may be seen from fig. 14b as an example of a 1300°C fictive temperature sample. The trend to the metastable equilibrium curve starts at 800°C and at 1000°C no isothermal volume change is detected within the time of measurement.

b) Between 750 and 950°C a tendency of volume contraction is observed in samples of natural silica glasses in the first expansion curve after quenching (fig. 14). The higher the fictive temperature the larger is this effect. The same is true for artificial silica glass at lower temperatures (500–700°C, fig. 14b). These contractions may be attributed to the relaxation of internal structural stresses produced by quenching, because these contractions almost disappeared in the second expansion curves. It is suggested that the relaxation process in this temperature range is partly connected with a healing process for "open bonds" and that during the first heating up chance



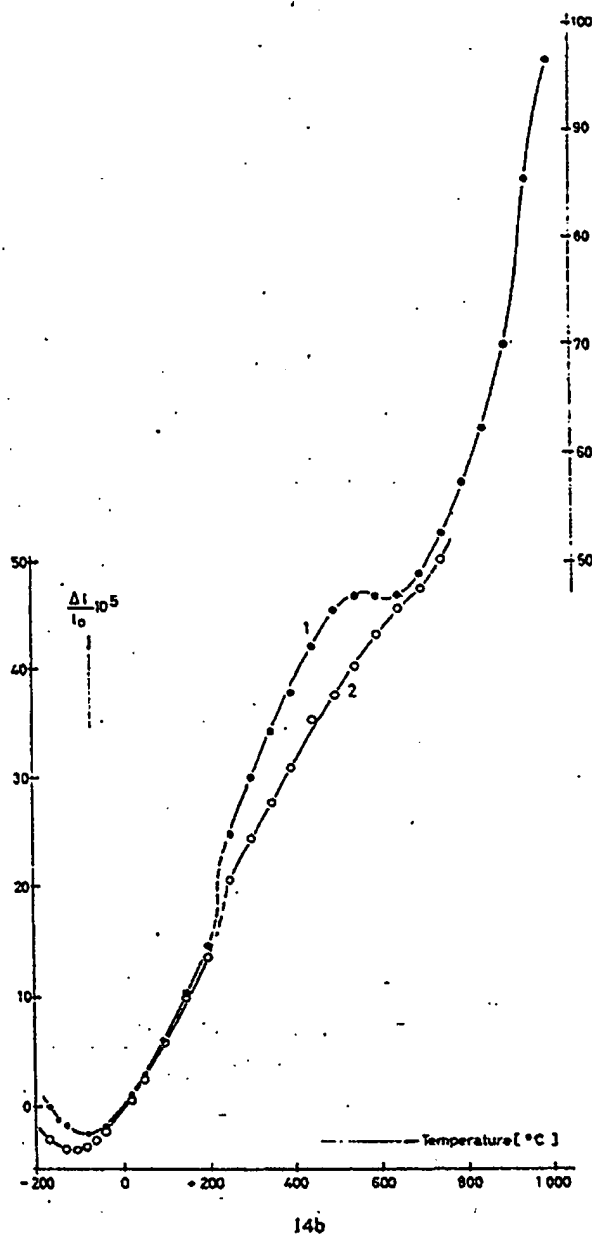


Fig. 14. Thermal expansion curves of type I/II (a), and type III silica glass (b), quenched from fictive temperatures of 1400°C (a) and 1300°C (b).

occasional linking of Si-O bonds by regroupings of SiO_4 -tetrahedra occurs.

Accordingly, it should be pointed out that in silica glasses there is the possibility for compression stresses as well as for tension stresses in the outer part of a sample, and vice versa for the interior part. If a sample is quenched from temperatures above 1550°C , the usual permanent stress distribution is built up by the latter contraction of the interior rather than the outer part. This produces tension in the temperature range of possible flow in the interior, and a compressive stress in the outer part. But if a sample is quenched from below 1550°C in a not too rapid manner, the latter expansion of the interior part in comparison to the outer one (see fig. 2) produces, by flow in the corresponding temperature range of low enough viscosity, a compression stress in the interior and a tension stress in the outer part.

c) A third volume relaxation of quenched samples is found in the temperature range of 200 – 300°C . The characterization of this volume change is the relatively large amount of change, the short relaxation time and the disappearance after reheating and slow cooling of the samples. There are two further characterizations, first, that these volume changes are only found in samples which were quenched from temperatures below 1550°C , and secondly, that the natural silica glasses show a contraction whereas the artificial silica glasses show a dilatation (figs. 14a and 14b). Again the relaxation time is shorter for the latter than for the former, possibly due to the high OH-content. It is remarkable, that the relaxation times in this low temperature range are shorter than those at 1000°C ; for example, the mean relaxation times for a natural silica glass at 1000°C are extensively larger than 1000 sec, whereas at 200 – 300°C they are distinctly smaller than 1000 sec. The relaxation process is a very complicated one and cannot be described by only one mean relaxation time⁷³⁾.

Some indications predict that also at 500 – 600°C volume changes take place⁷³⁾. Although this effect is small as compared to that at 200 – 300°C , however, it is not definite that the real effect is also small. This effect is only small in the sense of the sensibility of the thermal expansion measurements and of sample condition, because the volume relaxation at 500 – 600°C is only measurable after that at 200 – 300°C , which causes a decrease in the sensitivity for volume relaxation by a partly healing process in the form of a destruction of internal structural stress caused by transition processes^{75, 84)}.

An interpretation of the complex volume behaviour (sections 4.1 and 4.2) was attempted in the following manner⁸⁴⁾ with the help of temperature or density fluctuations and by the existence of preordered regions. Suppose, in the temperature range between the melting point of cristobalite and about 150°C below the melting point these fluctuations lead to agglomerations of $\text{SiO}_{4,2}$ -tetrahedron fragments having properties very similar to those of the

corresponding crystalline phase. These heterophasic* fluctuations could be understood from a statistical point of view in the sense of "embryos" after Volmer and Weber⁸⁶, and Fischer, Hollomon and Turnbull⁸⁷, being very small and having a high degree of disorder so that by X-ray diffraction no crystallinity will be detectable.

With the help of the postulate of preordered regions the complex volume behaviour may be interpreted**.

a) The branch of the negative thermal expansion (1550–1000°C) may be connected to the negative expansion coefficient of cristobalite in this range; that means, the preordered regions are very similar to cristobalite. Above 1550°C a "thermal decomposition" or a "premelting" of the preordered regions takes place and the volume temperature curve behaves normally. The "water"-content of the synthetic silica glasses causes a lower viscosity (see section 5.4.) and therefore a lower premelting temperature.

b) The contractions of the natural silica glasses at 200–300°C will be due to the volume shrinkage of the rapidly quenched preordered regions which will still have "high temperature modification" character and which have the chance, on slow heating during the measurement, to change to the "low-temperature modification"†. The observed volume expansion instead of a contraction in the synthetic silica glasses is attributed to the looser and more open structure and to the higher mobility of the tetrahedra caused by the "water"-content. Therefore the high-temperature preordered state will not be frozen in by quenching as in the case of the natural silica glasses and so a slight and rapid expansion occurs instead of a shrinkage.

c) The negative expansion at low temperatures may be a result of a preferred oscillation of the bending (transverse) vibration mode opposed to longitudinal vibration modes⁸³ (see last paragraph of section 4.1). The shift in the minimum temperature region with thermal history (–135 to –60°C) seems to be connected to internal structural stresses caused by the quenching process and to the more or less open structure with a different degree of open bonds.

4.3. VOLUME AND PRESSURE

The effects of pressure on glasses can be divided into three categories. First, the applied pressure on the glass below the glass transition temperature

* The concept "heterophasic" should be understood not in the classical thermodynamical sense, but in the sense of the statistical theories of fluctuations⁸⁵, where the one phase is the undercooled melt and the other one the preordered regions.

** For a more detailed discussion it is referred to ref. 84.

† Instead of the expression "modification" it would be better to say "preordered state", or high- or low-temperature preordered state respectively; instead of transformation point: transition range etc.⁸⁴)

may be low enough for reversibility of the density to be guaranteed; this behaviour is characterized by the volume compressibility. The pressure range of reversibility is strongly dependent on the kind of the pressure cell in question or on the amount of applied shear⁹⁴). The better the isostatic condition is realized the larger is the pressure range of volume reversibility (fig. 17). The best isostatic conditions are obtained by a silver chloride cell or by any liquid pressure cell.

Second, the applied pressure or the amount of the shear component is large enough to produce "irreversible" or "permanent" (with regard to low enough temperature) volume changes (densification) of glasses in the rigid state.

Third, the glass may be compressed at or above the glass transition temperature where the volume relaxation times are usually shorter: Here, large increase in density is possible under relative low applied pressures (below 10 kbar). Cooling under pressure makes the densification "permanent" if the end temperature is low enough.

a) *The reversible volume changes* may be expressed by the mean coefficient of compressibility^{88, 89}):

$$\beta_m = a(T) + b(T)p, \quad \beta_m = \frac{1}{V_0} \frac{V_0 - V_p}{p - p_0},$$

$$a(T) = (26.43 - 0.0025 T) \times 10^{-7} \text{ cm}^2/\text{kP},$$

$$b(T) = (43.6 - 0.080 T) \times 10^{-12} (\text{cm}^2/\text{kP})^2,$$

where T is in °C.

These data are valid in the temperature range of 22–260°C and in the pressure range of 0–3000 kg/cm². Up to 12 kbar no permanent volume

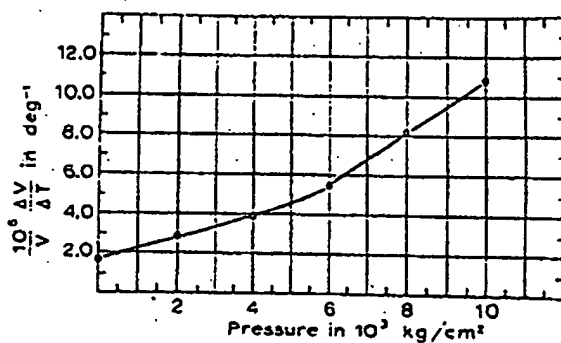


Fig. 15. Thermal expansion coefficient of silica glass between 11 and 390°C as a function of pressure calculated⁹⁰) after compressibility measurements⁹¹) in the reversible range of volume and pressure.

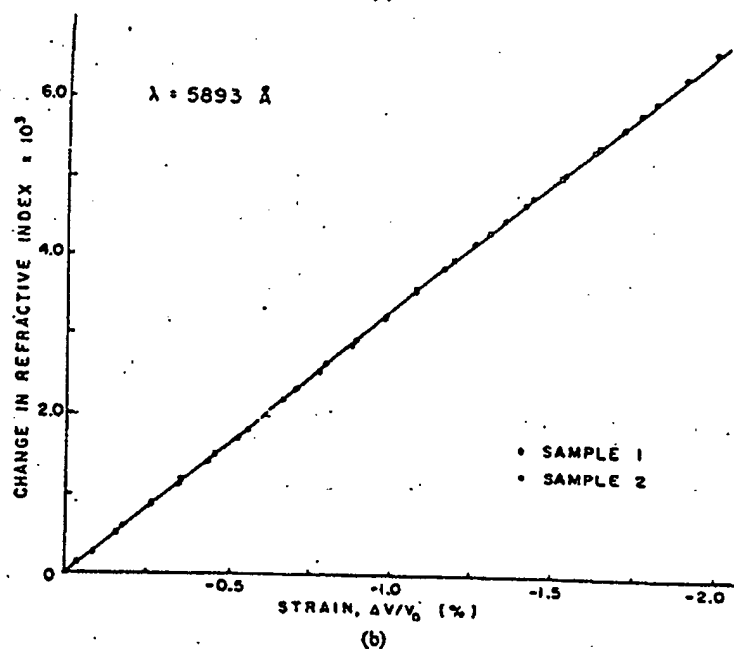
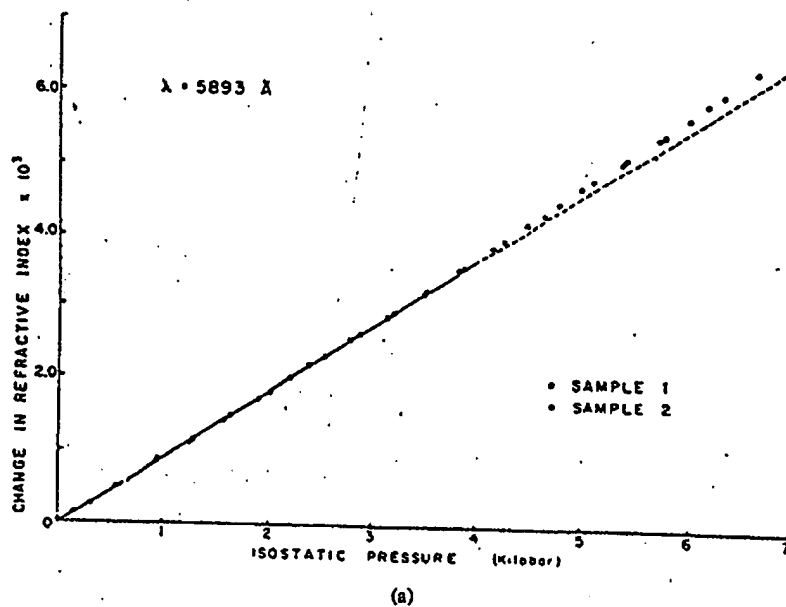


Fig. 16. Change of refractive index as a function of pressure (a) and strain (b) in the reversible volume-pressure range¹².

change was detectable. As a result, vitreous silica is also unusual in its compressibility behaviour because its compressibility increases with pressure whereas that of quartz and most other substances decreases with pressure. Remarkable is also the decrease of the pressure dependency of β_m with increasing temperature. This gives rise to a marked increase in the thermal expansion coefficient with increasing pressure as is calculated and shown in fig. 15^{90,91}).

It might be supposed that a normal negative pressure dependency will occur from a certain temperature upwards. Also, from a certain compression onward where the density of cristobalite is reached, a normal pressure dependence might be expected, because cristobalite, and also quartz, behave normal.

Further the actual strain produced in vitreous silica is higher than the value calculated from linear elasticity theory. Also, the change of refractive index of vitreous silica, with pressure is nonlinear above 4 kbar (fig. 16a)⁹² but exactly reversible. If the change of refractive index is plotted over the Lagrangian strain, linearity is obtained over the pressure range up to 7 kbar (fig. 16b). From this it follows in connection with Mueller's theory of photo

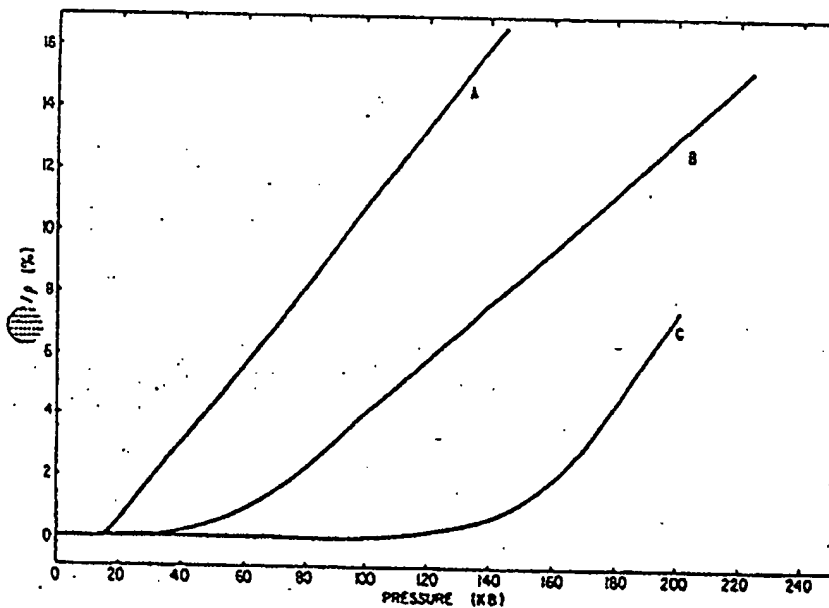


Fig. 17. Irreversible volume changes at room temperature caused by different types of pressure cells⁹⁴. (A) high shear component⁹⁵; (B) low shear⁹⁶; (C) very low shear component⁹⁷.

elasticity⁹³), that the voids in vitreous silica are gradually being filled when the medium is elastically compressed. The most probable mechanism may be the gradual movement of some of the voids surrounding oxygen ions by a preferred displacement of the oxygen ions towards the voids in connection with the transverse optical vibration modes of the Si-O-Si bond^{101,102}).

b) At higher pressures, with more or less shear stress components, *irreversible volume changes* take place up to 15% densification even at room temperature (fig. 17). At higher temperatures the densification process is facilitated, for instance at 400°C a permanent volume change of 14% at a pressure of 80 kbar, of 4% at 60 kbar and no change at 40 kbar is observed in a silver chloride cell⁹⁴), whereas no change at 80 kbar pressure is obtained at room temperature. The mechanism of densification is mainly connected with "flow" under shear action (fig. 18)⁹⁴). First the material undergoes elastic shrinkage. At higher, not entirely isostatic pressure, rupture of some SiO bonds is produced. The compression in conjunction with a shear stress leads to an interlocking of two parts of the network; this can be attributed to variations in the mutual orientation of SiO₄ tetrahedra.

The densification process is influenced by the impurities of vitreous silica. At a constant pressure of 50 kbar at 500 and 600 °C, the densification increases in the following manner: Type IV (Suprasil W) → type III (Suprasil) → type I (Infrasil)⁹⁷). This behaviour may be attributed to the more open

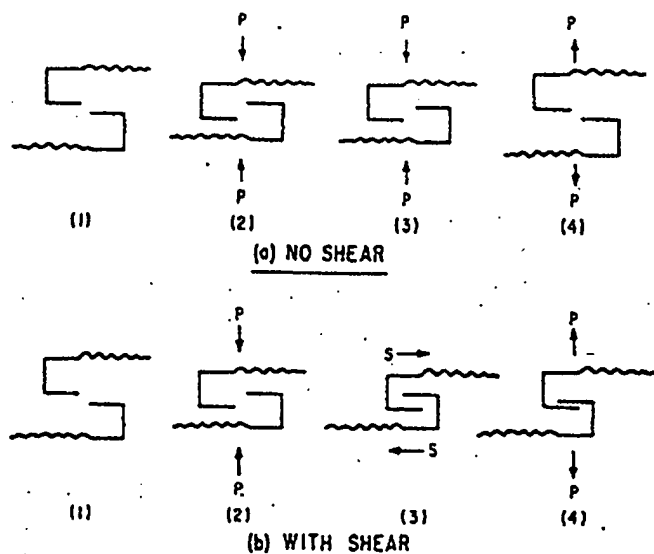


Fig. 18. Possible role of shear on densification of rigid glass (schematic)⁹⁴).

structure of Suprasil due to the high hydroxyl content (1200 ppm) as compared with Suprasil W (250 ppm Cl). However this does not hold for Infrasil. But, obviously, the higher content of metallic impurities, and the oxygen deficiency of Infrasil (240 nm absorption), may affect a densification much more strongly than do hydroxyl groups.

The annealing or the volume expansion with time at atmospheric pressure is a very complex process as shown in figs. 19 and 20⁹⁴). At the beginning of annealing, a rapid volume increase within a few minutes is observed. The higher the annealing temperature, the higher is this first volume increase. Later, the rate of volume change decreases markedly. The annealing process is dependent on the mechanical and thermal history. A densified sample, partly annealed at 500°C, shows another annealing behaviour when further

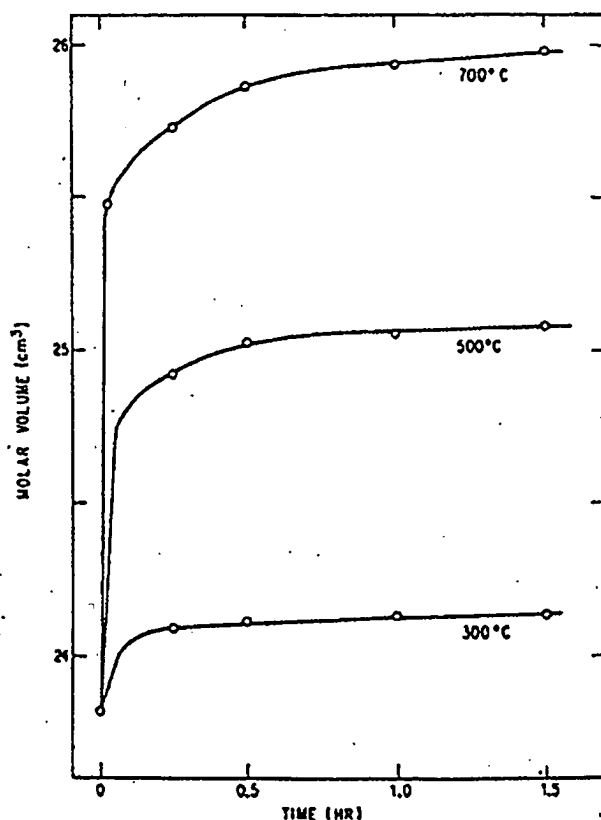


Fig. 19. Annealing of densified silica glass of $V_0 = 23.83 \text{ cm}^3/\text{mole}$ at 300, 500 and 700°C⁹⁴).

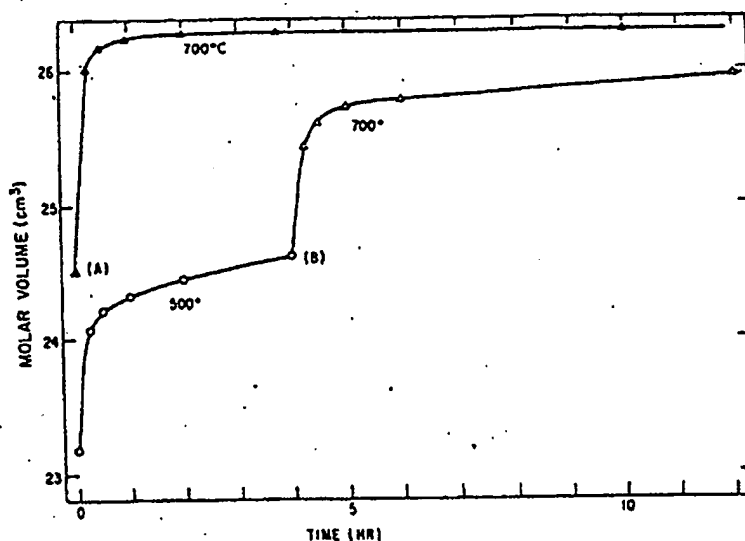


Fig. 20. Annealing of two specimens of densified silica glass. Effect of thermal history on initial annealing behaviour at A and B⁹⁴).

annealed at 700°C as compared to a less densified sample which was not pre-annealed at 500°C (fig. 20) in spite of the fact that the starting point is the same for both samples (A and B) before the treatment at 700°C.

Usually, the rate of the first volume increase is the higher the larger the densification. The extent of internal deformations of the network under the applied high pressures is seen from the fact that at the surface of samples, with densities above 2.33 g/cm³, cristobalite is formed during annealing at a temperature as low as 500°C.

An estimation of the activation energy of internal "flow" from initial slopes of the annealing curves gives surprisingly low values of 1–10 kcal/mole⁹⁴). A further phenomenological treatment of the second part of the annealing curves by a mathematical formalism of a distribution (spectrum) of activation energies leads to somewhat higher values ranging from 34 to 76 kcal/mole with a sharp maximum at 41 kcal/mole and two broad maxima centred at about 54 and 70 kcal/mole⁹⁸.) All values are considerably lower than the activation energies of viscous flow. Care must be taken of the physical significance of these data, but an indication may be given that the comparatively low activation energies can be interpreted as being mainly due to reorientations of SiO₄ tetrahedra with occasional linking of Si–O bonds taking place during annealing in contrary to real viscous flow.

Measurements of microhardness on densified silica glasses of type III at room temperature show interesting irregularities at those densifications (varying from 2.2021 to 2.567 g/cm³), corresponding to the densities of cristobalite, quartz, keatite and stishovite. Also the refractive index shows a similar relation to these modifications⁹⁹). This fact is of interest with regard to the concept of preordered regions (section 4.2.). For still higher pressures (up to 120 kbar) and temperatures at which a transition to the crystalline modifications (quartz, coesite, stishovite) takes place, the reader is referred to Stöller and Arndt⁹⁹).

c) Densification near and above the glass transition temperature is already obtained at pressures as low as, for instance, 114 bar (fig. 21)¹¹). At a tempe-

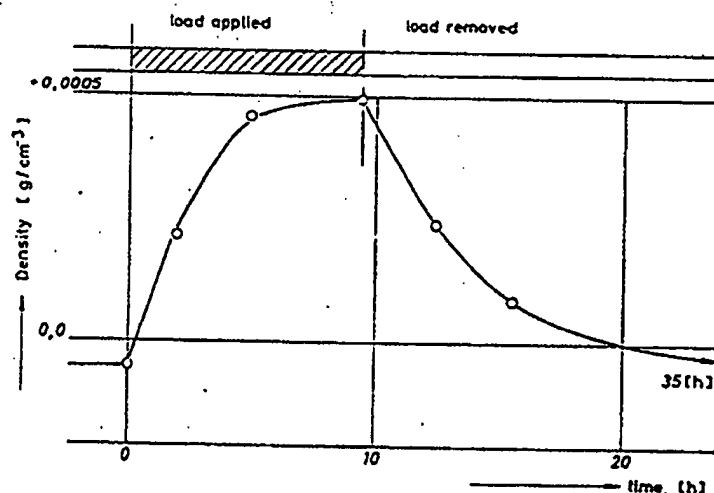


Fig. 21. Densification by a pressure of 114 atm. at 1080°C and annealing of silica glass at 1080°C¹¹).

perature of 1080°C a densification of 5×10^{-4} g/cm³ is reached after 10 hr which can be frozen in by cooling under load. Relaxation of the compressed volume without load at the same temperature is maintained after nearly another 10 hr in the manner of a viscoelastic body.

If the annealing process of a silica glass densified above the glass transition temperature is made at temperatures below the glass transition temperature, the relaxation process is more complex and differs considerably from that of a glass densified below the glass transition temperature. The most significant difference of both densification mechanisms is the minimum annealing temperature at which isothermal volume flow is observed¹⁰⁰). In table 1 a

TABLE I

Comparison of minimum temperature T_0 at which annealing is observed in 30 min for densified glasses¹⁰⁰.

	Glass transition temperature (°C)	Minimum temperature (°C)	
		In rigid state densified glass	In non-rigid state densified glass melt
B ₂ O ₃	230	25	150
SiO ₂	1200	200	700

comparison between this minimum temperature is listed for densified SiO₂ and B₂O₃-glass whereby the annealing time of 30 min is arbitrarily chosen.

In the case of silica densifications of 100 $\Delta\rho/\rho = 3.71$ to 3.76 were measured at 1600°C and 15 kbar, in the case of B₂O₃ a densification of 5.80 at 650°C is obtained at 15 kbar and of 7.50 at 900°C at a 20 kbar pressure¹⁰⁰.

For a structural consideration these results show that the amount of densification increases qualitatively with increasing free volume, viz. with increasing temperature, and further more, the densification process in the non-rigid state leaves far less open Si-O or B-O bonds than in the rigid state, because above the glass transition temperature the densification is accompanied by a real viscous flow, and during cooling under pressure, it is accompanied by a thermal healing process. Therefore the glass which is densified in the non-rigid state behaves more stable, below the glass transition temperature, than the rigid state densified glass.

4.4. ELASTIC AND INTERNAL FRICTION BEHAVIOUR

It is a well-known fact, that the elastic moduli also show anomalous behaviour in two points: the temperature coefficient and the coefficient of large longitudinal elastic strain (of fibers) of the elastic moduli are positive. The latter may be expressed by the experimentally determined expressions¹⁰³:

$$E = 7.33(1 + 5.75\varepsilon) \times 10^3 \text{ kg/mm}^2,$$

$$G = 3.21(1 + 3.06\varepsilon) \times 10^3 \text{ kg/mm}^2,$$

where E is Young's modulus, G is the rigidity modulus and ε the elongation.

This behaviour was not only measured on fibers but also on silica glass rods¹⁰⁴. This is a consequence of the positive pressure coefficient of the compressibility (see section 4.3a), viz. the equation

$$K = \frac{1}{\beta_m} = \frac{1}{a + bp} \sim a - bp = \frac{E}{3(1 - 2\nu)},$$

where K is the bulk modulus and ν Poisson's ratio, holds for compression stress, that means E must increase with increasing tensile stress. Therefore it will be referred to section 4.3a for a discussion on this point.

Both, Young's and the shear modulus versus temperature are increasing in the temperature range -200 to 1000°C ^{105,108,109}). Nearly linearity is found from 25 to 800°C . Near 60°K the moduli have a minimum¹⁰⁷) accompanied by an internal friction peak in the neighbourhood of 35°K at 50 – 100 kc/s. Above 60°K together with the moduli (Young's and shear) also the Poisson's ratio increases continuously with increasing temperature.

The increase in Young's modulus is in a qualitative way most easily interpreted as being analogous to the case of rubber stretching^{104,108}). But also other interpretations were given, reducing the problem to the extreme low coefficient of expansion^{109,110}). Considering any modulus M as a function of volume V and temperature T , $M = M(V, T)$, the total temperature dependence is given by

$$\frac{dM}{dT} = \alpha V \left(\frac{\partial M}{\partial V} \right)_T + \left(\frac{\partial M}{\partial T} \right)_V,$$

$$\alpha = \frac{1}{V} \left(\frac{\partial V}{\partial T} \right)_P = \text{coefficient of expansion.}$$

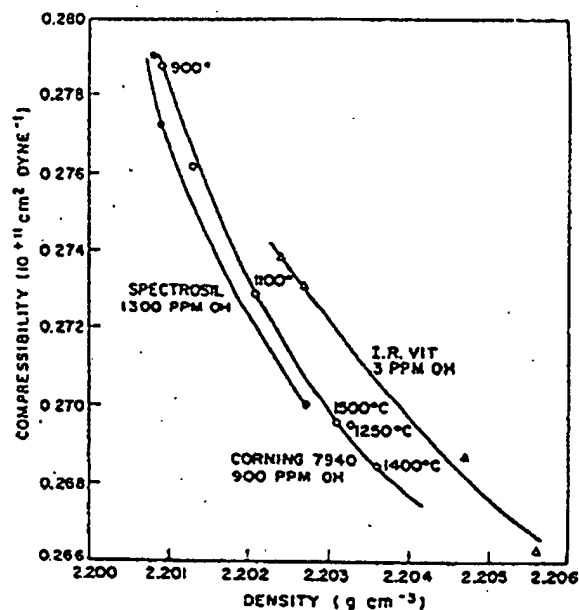
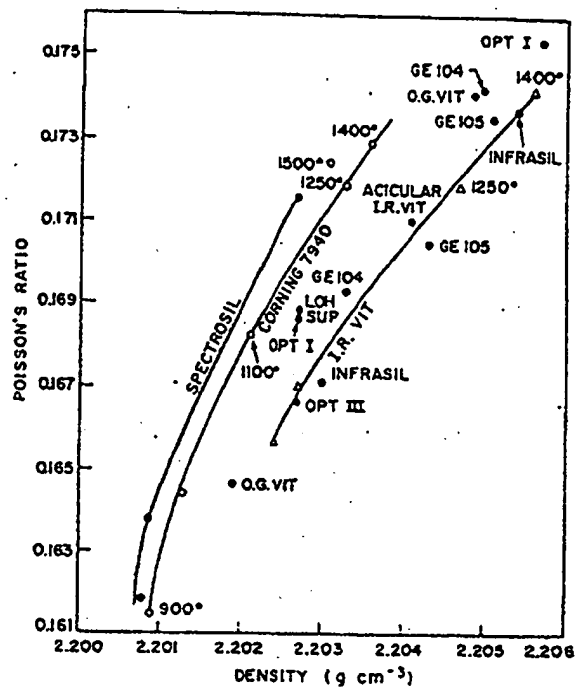
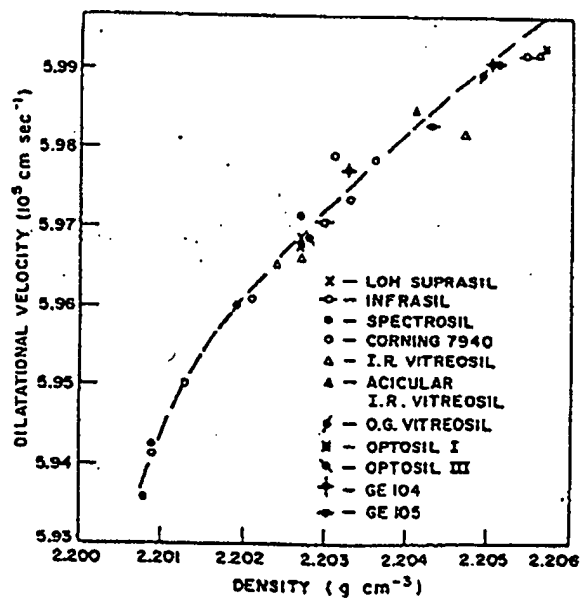


Fig. 22. Compressibility of three silica glasses as a function of density¹¹²).


 Fig. 23. Poisson's ratio as a function of density⁽¹¹⁾.

 Fig. 24. Dilatational velocity as a function of density for various silica glasses⁽¹¹⁾.

It follows from this equation that the sign of dM/dT will be governed by the sign of $(\partial M/\partial T)_V$, if α is negligibly small. As well in the case of a Born-von Kärman solid as in the case of a Debye and Grüneisen solid it was shown^{109,110}, that dM/dT is negative at low temperature and large α , and positive at high temperature and small α . For the positive temperature coefficient of M of silica glass the small thermal expansion coefficient plays two important roles: first, the small value of α eliminates the always negative volume term $(\partial M/\partial V)_T$ and second, at small α the pure temperature term $(\partial M/\partial T)_V$ becomes positive from a moderate temperature upward.

As a function of density, produced by thermal history and "water"-content, elastic properties measured at room temperature at acoustic frequencies show the following behaviour. The shear velocity, the shear modulus and the compressibility decrease with increasing density, whereas the dilatational velocity, the Lamé parameter λ and Poisson's ratio increase with increasing density¹¹¹) (figs. 22-25). While the behaviour of compressibility, Poisson's ratio and Young's modulus (from dilatational velocity and from the density itself and from the Grüneisen equation: $\beta c_p = \text{const.} \times \alpha V$, and from the Lamé parameter λ) is immediately well understood, an interpretation of the behaviour of the shear velocity and shear modulus seems to

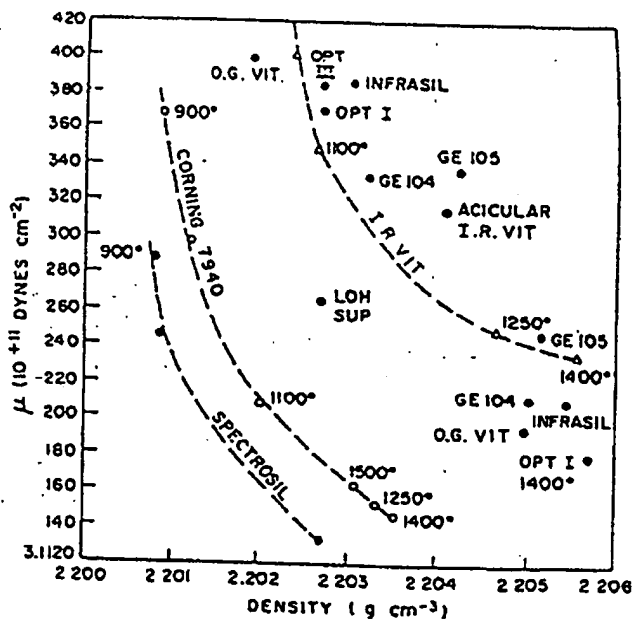
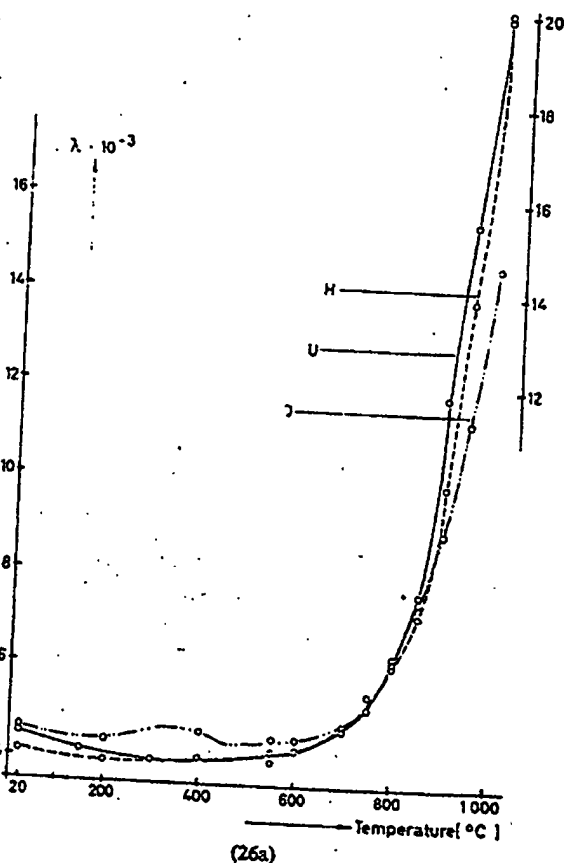


Fig. 25. Shear modulus (rigidity) as a function of density for a number of silica glasses¹¹¹).

be difficult, but it may be indicated that internal stresses in the quenched samples and open bonds or other kinds of inhomogeneities such as the preordered regions in the random glass network matrix section (4.2) may be responsible for the shear velocity dependence.

According to the general theory of dispersion any change of an energy-connected variable is related to an energy absorption peak. The deviation of Young's modulus from linear positive temperature dependency at 800 to 1000°C is connected with an increase of internal friction measured at about 10 c/s in air (fig. 26)⁷⁰). In this temperature range the low temperature side of the glass-transition-internal-friction peak is noticeable. Structurally, this friction loss is related to the initial break-down of the polymer network from a rigid glassy state to an undercooled liquid metastable state. As in many other cases again a marked difference is found between the "water"-rich



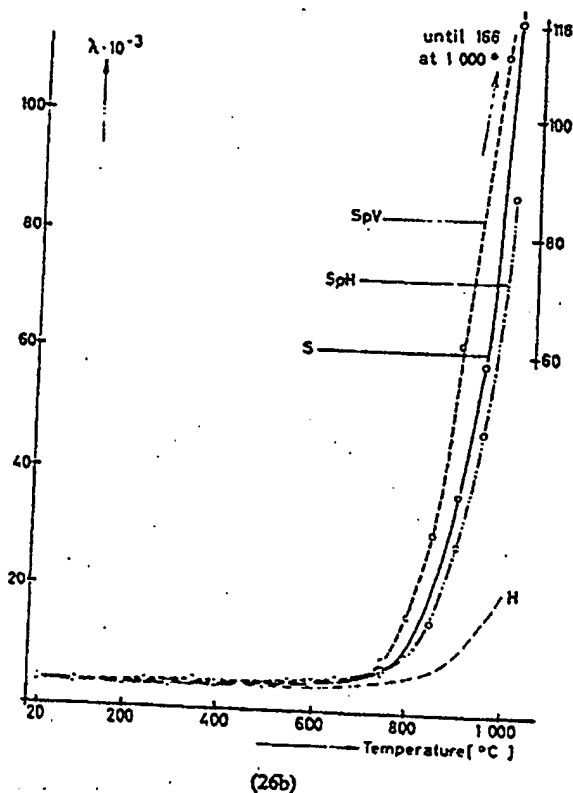
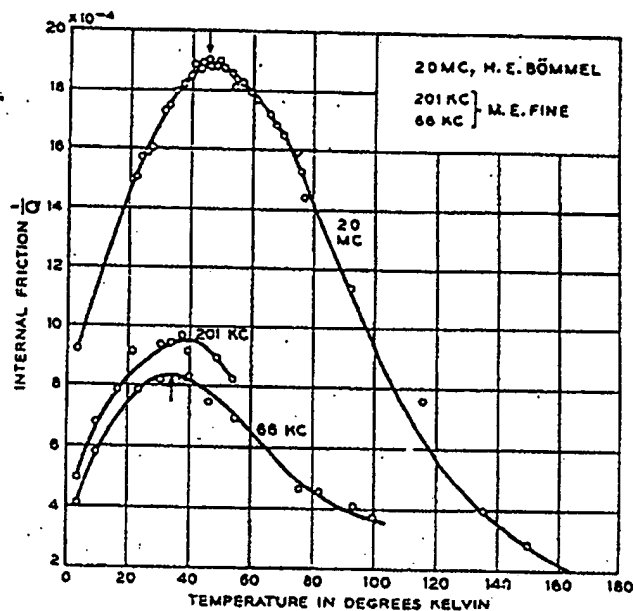
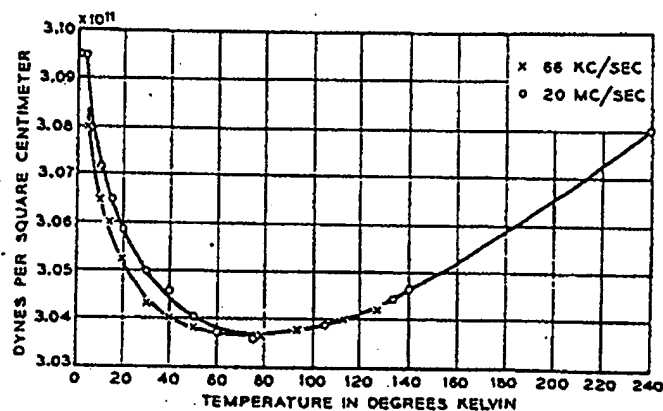


Fig. 26. Internal friction of type I/II and of type III silica glasses (b) as a function of temperature (fictive temperature = 1300°C). H = Homosil, U = Ultrasil, I = Infrasil (types I/II); S = Suprasil, SpV = Spectrosil, SpH = Spectrosil H (types III).

artificial and the "water"-poor natural silica glasses (type I/II). The higher "water"-content of the type III silica glasses causes a shift in the glass-transition temperature to lower temperatures. Here an example exists where silica glasses show a similar behaviour as multi-component silicate and other oxide glasses. The influence of OH-content on internal friction in the glass-transition range is closely connected to the viscosity (see section 5.4), which is lowered considerably by the incorporation of OH-groups.

At very low temperatures and high frequencies (ultrasonic, longitudinal waves in the kc/s and Mc/s range) another internal-friction peak is observed together with a minimum of rigidity^{107,112}). The peak and also the minimum of rigidity shift to higher temperatures with increasing frequencies (figs. 27


 Fig. 27. Internal friction peak at low temperatures at different frequencies¹¹²).

 Fig. 28. Rigidity at low temperatures at different frequencies¹⁰⁷).

and 28) indicating that the mechanical losses are due to a relaxation mechanism. It has been demonstrated by analysis that a particular distribution of activation energies, each of which associated with a relaxation time would account for the shape of the experimental curves¹¹²). It is remarkable that the absorption does not occur in the corresponding crystalline quartz struc-

ture. The amount of the measured activation energy of 1.03 kcal/mole will be too small for an atomic diffusion process or for a molecular rotation, but too large for the absorption of a shear elastic wave. Therefore the losses are interpreted¹¹²⁾ as being due to Si-O-Si bond deformation vibrations of those oxygen atoms having alternative positions of equal energies. This hypothesis is confirmed by the successful extrapolation of the relaxation frequencies from the ultrasonic range at low temperatures (35 to 48°K) to the Raman frequency of 30 cm⁻¹ at room temperature after the Eyring-type equation

$$\tau_0 = \frac{kT}{h} e^{-q/RT} \quad \text{with } q = 1.03 \text{ kcal/mole.}$$

Again, differences were observed between type I and type III silica glasses. The temperature of maximum ultrasonic loss is 43.5°K for an Infrasil "water"-free and 47.5°K for a Suprasil synthetic silica glass containing about 10³ ppm OH ions, both samples measured at a frequency of 20 Mc/s (longitudinal)¹¹³⁾.

It could be confirmed by recent measurements and by an extend on other fundamental oxide glass formers like GeO₂, B₂O₃ and As₂O₃¹¹⁴⁾, as well as sodium germanate glasses¹¹⁵⁾, that the low temperature internal friction effect is attributed to a relaxation of transverse vibrating bridging oxygen atoms¹¹²⁾ in spite of the fact that also a two-bond-length model, based on studies of fast neutron irradiated specimens of silica glass, involving a longitudinal motion of bridging oxygen atoms which have two stress-sensitive equivalent equilibrium positions, can explain the effect¹¹⁴⁾.

4.5. HEAT CAPACITY AND HEAT CONDUCTION

According to the expression for the temperature dependency of specific heat

$$c_v = 3R \sum E_i(X_i),$$

in which E is the Einstein function

$$E(x) = x^2 e^x / (e^x - 1)^2,$$

where

$$x = h\nu/kT = \theta/T,$$

h =Planck's constant, ν =frequency of proper oscillation, k =Boltzmann's constant, R =gas constant and θ =Debye temperature, Smyth and co-workers¹¹⁶⁾ calculated the specific heat of vitreous silica and showed that best agreement with experimental values is obtained (fig. 29) if the following three characteristic temperatures are chosen: $\theta_1=1100^\circ\text{K}$ for each of the

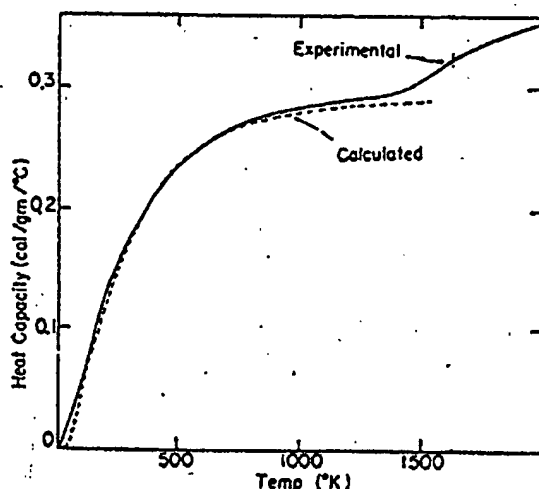


Fig. 29. Heat capacity of vitreous silica as a function of temperature. Solid line: measured¹¹⁷; dashed line: calculated¹¹⁸.

three silicon vibrations, $\theta_T = 370^\circ\text{K}$ for each of the three transverse oxygen vibration modes, and $\theta_L = 1220^\circ\text{K}$ for each of the two longitudinal oxygen oscillations; the θ_i correspond to vibrations in the infrared range of 23×10^{12} , 7.7×10^{12} and 25.4×10^{12} c/s.

The experimental data in fig. 29, composed by Sosman¹¹⁷, show a discontinuity at about 1100°C . It is remarkable that not all authors have measured this increase. Possibly, this increase of the heat content is of structural origin and may depend on thermal history, because in this temperature range the glass transition of silica takes place. Similar to the increase of the heat content at the transformation of a crystal to its melt, also an increase may be expected, when a glass is heated across the transition temperature, which is called the "regrouping" heat by some authors¹¹⁸, because endotherm peaks in differential thermoanalysis of some glasses were measured.

It is of further interest to note, that an excess specific heat of vitreous silica exists at very low temperatures¹¹⁹, whereas no such excess is observable in quartz and other crystalline substances. This excess heat is the difference between C_p measured, and C_p calculated from the Debye temperature and the elastic constants:

$$\begin{aligned} C_{p(\text{excess})} &= C_{p(\text{meas.})} - C_{p(\text{calc.})} \\ &= C_{p(\text{meas.})} - SD \left(\frac{\theta_{(\text{elastic})}}{T} \right), \\ C_{p(\text{meas.})} &\sim 2 \text{ to } 5 \times C_{p(\text{calc.})}, \end{aligned}$$

where

$$\theta_{(\text{elastic})} = \frac{h}{k} \left(\frac{n}{4\pi V_c} \right)^{\frac{1}{3}} c_m,$$

h = Planck's constant, k = Boltzmann's constant, c_m = mean sound velocity determined from the density and the elastic constants, n = number of degrees of freedom per cell for lattice vibrations, V_c = volume per cell, $D(\theta/T)$ is the Debye formula and $S=3R$ for Si-O-Si, or $S=\frac{9}{2}R$ for the SiO_4 tetrahedron as a vibrational unit. Although no exact explanation can be given for the excess specific heat at temperatures below 20°K , especially below 5°K , it is important that, in a qualitative way [inconsistent with lattice dynamics¹²⁰], a model in which the Si-O-Si bending vibrations can be made responsible for all the low-temperature specific heat¹¹⁹) and that all of the frequencies required to account for this heat capacity are to be found in the region of optical modes of very low frequencies with an intense continuum extending from 560 cm^{-1} down to 8 cm^{-1} as can be shown directly by the Raman spectrum and the Brillouin scattering spectra of silica glass^{121,122}).

A characteristic difference between the vitreous and crystalline state is evident through the temperature dependence of heat-conduction (fig. 30).

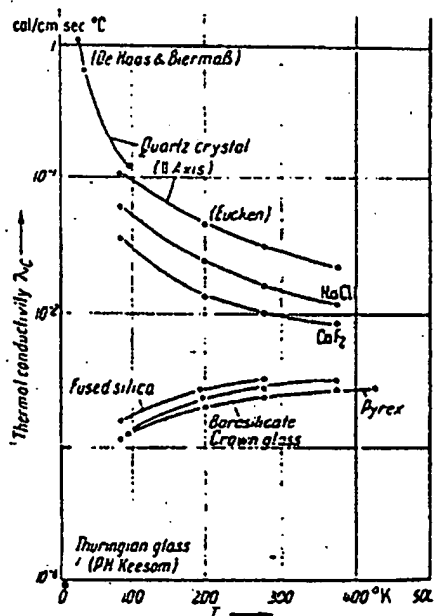


Fig. 30. Thermal conductivity in crystalline and glassy materials^{123,124}).

In analogy with the photons in optical energy transport, the conception of the phonons (high frequency thermoelastic lattice waves), with certain mean free paths, proved important in heat conduction problems (phonon conduction). The longer the mean free path l , the higher the thermal conductivity λ_{th} :

$$\lambda_{th} = \frac{1}{3} c v l, \quad q = -\lambda_{th} \Delta T / \Delta x,$$

where c is the heat capacity per unit volume, v the average sound velocity, q the rate of heat transfer through a unit area per unit time, and Δx the space between the temperature drop ΔT . According to the regular atomic arrangements in crystal layers the crystals have large l -values at low temperatures and therefore a great λ_{th} . The lack of periodicity and symmetry of a lattice in glasses causes large interchange energies between thermoelastic waves such that the mean free path, l is short. It is stated¹²⁵) that in case of glasses l is constant, independent of temperature, except for long wave lengths at low temperatures. Therefore λ_{th} is widely proportional to the specific heat at most temperatures. This is shown for silica glass in fig. 31¹²⁶) for tempe-

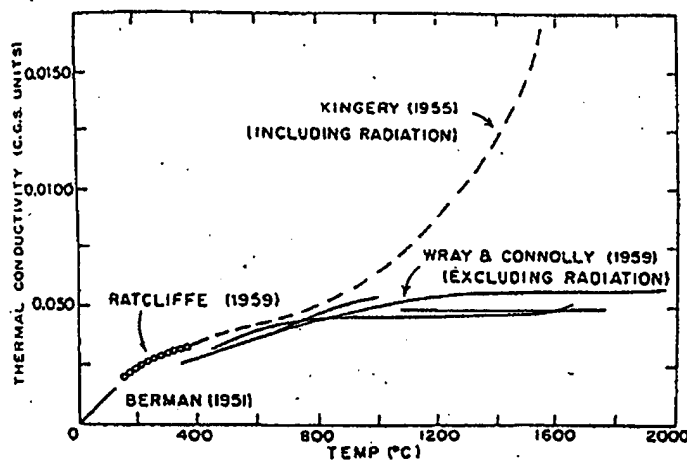


Fig. 31. Thermal conductivity of silica glass at high temperatures¹²⁶).

atures above room temperature. Here, the radiation conductivity (photon conduction)

$$\lambda_r = \frac{16\sigma n^2 T^3}{3\kappa},$$

(σ =Stefan-Boltzmann constant, n =refractive index, and κ =absorption coefficient) is eliminated (difference between dashed and solid line)¹²⁷.

The proportionality between λ_{th} and c_p is valid to temperatures as low as liquid-oxygen temperature. At lower temperatures the conductivity decreases more slowly corresponding to an increase in mean free path of the low-frequency thermal waves. In general this is plausible because the disorder of the silica network becomes less important for longer wave lengths. But a more sensitive analysis at temperatures below 20°K have led to difficulties in interpreting the higher values and the "knee" in the thermal conductivity curve around 10°K (fig. 32). These were overcome by assuming a much

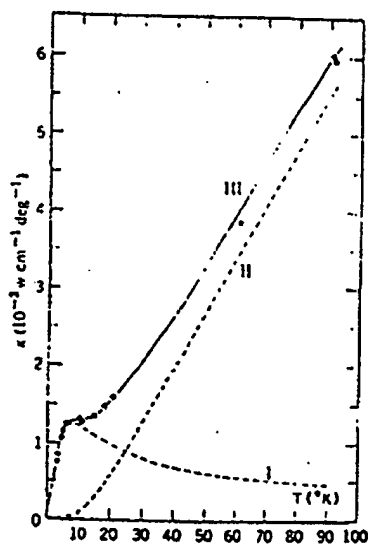


Fig. 32. Thermal conductivity of silica glass at very low temperatures, calculated (curves I, II, III)¹²⁵ and measured¹³⁰. Explanations see text.

longer mean free path for the longitudinal than for the transverse waves^{129,130}: At high frequencies and temperatures, a strong interaction between the two polarization branches, by means of three-phonon processes, result in an effective mean free path of the longitudinal waves, which is nearly the same as that of the transverse waves. This results in a conductivity, given by curve II of fig. 32. At lower frequencies the three-phonon processes are not sufficiently numerous to tie the mean free path of both, longitudinal and transversal, waves. This leads to completely uncoupled longitudinal waves with lengths very much longer than those of the transverse waves,

giving rise to an additional conductivity proportional to T in the range of 0–5°K. Above this temperature the partial coupling causes a decrease (curve I) and the superposition leads to the measured “knee” of the total conductivity (curve III). As in some foregoing sections (4.1 and 4.4), it is remarkable that the available experimental data cannot be explained without the assumption that very low frequency waves exist in both the optical and the acoustical branch.

Besides thermal fluctuations, also defects and voids with low-frequency mechanical resonances are to be considered giving rise to spin-“lattice” interactions and relaxations, and to unusual scattering of phonons which influence the short mean free path especially of the transverse phonons¹³¹. Therefore, a dependence of thermal conductivity, on thermal history and on type I/II as well as on type III silica glasses, is to be expected, and possibly vice versa, from that information on the structural defects.

4.6. STRENGTH

The expression “strength” usually refers to the tensile or bending strength of a material. It is obvious that this property depends on the weakest part of the material and this is mainly the surface, because the surface will be attacked chemically or mechanically. Surface flaws are usually cracks. A glass surface, which was thoroughly fire-polished or etched by hydrofluoric acid, should be free of cracks and should have theoretically maximum tensile fracture strength of $\frac{1}{2}$ of Young's modulus. In the case of silica, this means a strength of about 1.43×10^3 kP/mm², or taking into consideration the relation $E = E_0(1 + \alpha\epsilon)$ from section 4.4, the intrinsic cohesive strength of vitreous silica is expected to exceed 2.25×10^3 kP/mm². The highest observed strengths reported for silica glass fibers are: 1.5 and 1.6×10^3 kP/mm²^{132,133}; the highest strength observed for bulk vitreous silica at 78°K is 1.38×10^3 kP/mm²¹⁰⁴.

The slightest mechanical damage, such as produced by touching the sample with dirty fingers, causes a serious weakening. Therefore, the usual values are around 600 kP/mm². The causes of surface damage are studied extensively and described in refs. 104 and 134. Here, only very briefly, should be listed the different types of strength lowering effects: cracks, crystallization, condensation and adsorption of fluids (especially water) and gases, stress corrosion, “static fatigue”, and volume fluctuations.

It seems, that a fluctuation process is a practical barrier in achieving the ultimate strength experimentally. But it was shown¹⁰⁴, that at a temperature of 78°K the fluctuations are unimportant and that further lowering of the temperature causes no apparent increase in ultimate strength. It can be concluded that the volume fluctuation processes are the reason why the

strength) in spite of the fact, that the air condition reduces the strength, as compared to vacuo and low temperatures, far more by surface attack and fluctuations than the indicated differences. This fact should give rise to the conclusion that the structure of a drawn fiber is different from that of the bulk glass. This seems to be confirmed in the literature on glass fibers of multi-component composition*, although, partly very inconsistent conclusions, and experimental suppositions, yet fiber drawing conditions and results were found. An analysis of the possible silica glass fiber structure was pointed out¹⁴⁰) which led to a model as pictured in fig. 34. This figure does

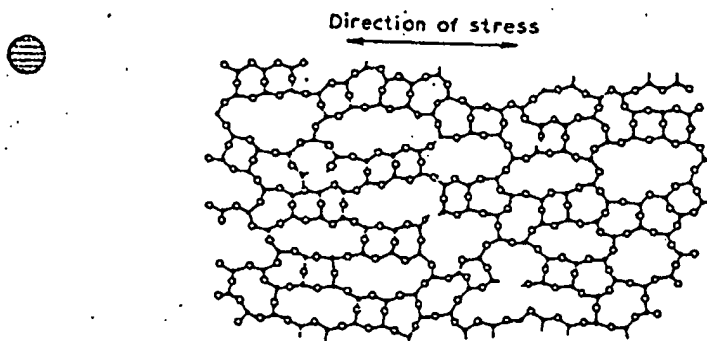


Fig. 34. Possible structure of silica glass fibers in regions of no preordered habitus.

not show the whole structure but that part of the deformed fluid-like structure without the preordered regions of section 4.2. It will be noted that there are three characteristic points differing from the isotropic structure: first, preferred orientation of silicon tetrahedra rows (double "chain-like") and deformation of the free volume in the drawing direction (arrow); second, the tetrahedra are distorted, slightly stretched in the drawing direction and slightly contracted perpendicular to it; third, the "broken" or "open" bonds may be partly of thermal and partly of mechanical origin. This picture is based on the anisotropy of silica glass fibers, of refractive index (birefringence $\Delta n \sim 270$ nm/cm of 12 μ m fibers), of density, of infrared absorption bands and of oriented crystallization (section 4.7).

4.7. CRYSTALLIZATION

Vitreous silica is one of the few interesting oxide glasses in which the composition of the crystalline phase is the same as the glass. Heterogeneous

* It is outside the scope of this article to consider that literature; the reader will be directed to refs. 108, 135-139, where also further literature will be cited.

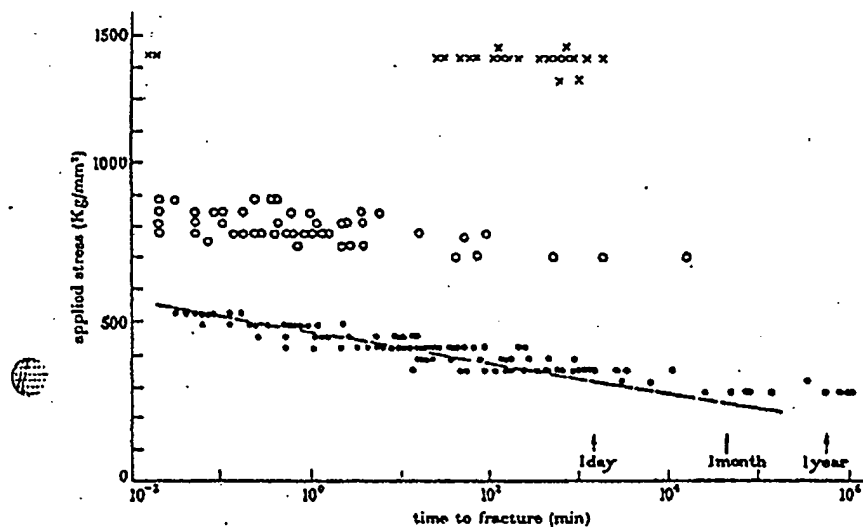


Fig. 33. Tensile strength and static fatigue of silica glass fibers at room temperature in air (●) and in vacuo (○), and at -196°C in vacuo (×)¹³³.

strength of silica glass increases with decreasing, and not with increasing, temperature as it could be expected according to the increase in Young's modulus.

Fig. 33 shows the features of the two main reasons of static fatigue of carefully prepared silica glass fibers (20 to 40 μm , drawn from a 1 mm diameter Vitreosil rod, i.e. type I silica-glass)¹³³; in vacuo at 78°K nearly no fatigue is observed, in vacuo at room temperature only about half of the strength at 78°K is observed, and fatigue is measured (fluctuation processes), and in air at room temperature, the strength is about $\frac{1}{3}$ that at 78°K and a stronger fatigue than in vacuo is observed (stress corrosion by water vapour)¹³⁴.

Regarding the ultimate strengths (at 78°K) of silica glass rods¹⁰⁴ ($1.38 \times 10^3 \text{ kP/mm}^2$) and silica glass fibers^{132,133} (1.5×10^3 and $1.6 \times 10^3 \text{ kP/mm}^2$), one might come to the conclusion, that the strength will be practically equal in both cases and the small difference will be due to the greater probability to get a flawless piece of silica glass in the case of fibers. But, if one compares the measurements at room temperature in air, not only between different author groups^{104,132,133}, but also among one and the same team¹³³, a similar difference is found between the strength of about 1 mm rods (580 for the ultimate and 520 kP/mm^2 for the most probable strength) and the strength of fibers (710 for the ultimate and 620 kP/mm^2 for the most probable

crystallization seems to be the only method to transform pure silica glass into cristobalite as the only modification. The heterogeneities are either surface or impurity centres.

Even under very pure furnace conditions, very pure vitreous silica crystallizes in the surface at, and above, 1100°C after sufficient long time. Measurable differences are to be expected between different silica glasses. It is also expected that the crystallization from the surface obeys a reaction law of zero order, i.e. the growth rate is constant (linear kinetics), and that the "water"-rich silica glasses will crystallize faster than type I/II silica glasses from the surface, whereas the latter will also crystallize from impurity centres if these are of sufficient concentration.

This concept holds true without one exception: the type I silica glasses ("water"-poor, electrically melted) have diffusion-controlled growth kinetics in both water vapour and in oxygen atmospheres¹⁴¹⁻¹⁴³. It is evident, that this behaviour is determined by oxygen deficiency and by the absence of structurally-combined water in this silica glass, i.e. in type I (SiO_{2-x} , where x is of the order of 10^{-4-5})⁵⁶, and that the growth mechanism is controlled by diffusion of oxygen bearing species too, and by the activation at the glass-crystal interface¹⁴². The observed growth rates at 1460°C in a 478 mm water vapour atmosphere are: 0.98 $\mu\text{m}/\text{min}$ for type III, and 132 $\mu\text{m}^2/\text{min}$ for an oxygen-deficient (SiO_{2-x}) silica glass which was prepared from type III by de-watering and melting with 70 ppm of silicon (the x -value being indefinite)*.

An increase of the crystallization rate is found with increasing temperature, of course, with increasing water vapour pressure (from a certain pressure on the growth rate proportional to the square root of water vapour pressure) in both types, and with increased oxygen pressure only in the non-stoichiometric silica glass, the influence of water vapour being larger, by a factor of more than two, than that of oxygen. In the absence of oxygen, the crystallization of the latter will also occur, but at a lower rate^{143,144}. It can be concluded, that an oxygen atmosphere is only important if there is an oxygen deficiency in the glass, and that a water vapour atmosphere is accelerating the crystallization in two ways: H_2O acts as a source of oxygen and as a

* The value of 132 $\mu\text{m}^2/\text{min}$ in parabolic form represents a slower mean diffusion velocity than the linear one of 0.98 $\mu\text{m}/\text{min}$, i.e. after the same comparable time the thickness of the crystallized layer will be larger in the linear case (0.98 $\mu\text{m}/\text{min}$) than in the parabolic case (132 $\mu\text{m}^2/\text{min}$). The crystallization rates, of type I silica glasses, are of the same order as that of the de-watered and reduced type III silica glass (100-200 $\mu\text{m}^2/\text{min}$ at 1460°C and 480 mm water vapour pressure) depending on the impurity content other than OH and on the degree of oxygen deficiency. It is remarkable that a type IV silica glass (Corning 7943) shows also parabolic growth kinetics (about 30 $\mu\text{m}^2/\text{min}$ only), that means, it was produced under reducing conditions¹⁴¹.

source of weakening the glass structure by the incorporation of H_2O ; nearly each molecule forming two hydroxyl groups causes rupture of a Si-O bond.

In table 2 a comparison is given between different crystallization conditions of a de-watered type III silica glass for a temperature of $1486^\circ C$ after Wagstaff et al.^{141,142}.

TABLE 2

Atmosphere	Crystallization rates ($\mu m/min$) from surface
452 mm H_2O	1.02
Dry N_2 or O_2	0.42
Vacuo	0.12

The addition of only 0.32 wt% Na_2O causes an increase of the crystallization rate up to $670 \mu m/min$ at the temperature of maximum crystallization rate ($1400^\circ C$)¹⁴⁵. This shows the effect of impurities, which in turn, greatly intensify the needed mobility for crystallization. In connection with the concept of the preordered regions this mobility is well understood⁸⁴.

Now, the question arises as to what the true crystallization rate of silica glass is. In high purity silica glass (type II to IV) no crystallization in the interior of the bulk glass could be observed. But recently in Vitreosil (type I) internal devitrification, heterogeneously nucleated by very small impurity regions (of the order of a few microns), has been observed¹⁴⁴. This fact is important in a twofold way: firstly, high-cristobalite crystals are obtained metastable, below their normal transformation temperature even down to liquid helium temperature, as a result of the tensile stresses developed across the boundary during cooling; and secondly, intrinsic growth rates can be maintained to allow the possibility of repeated increments of crystal growth to be measured on the same growing crystal, as long as the cristobalite does not transform. On cooling some crystals change to low cristobalite, and if the tensile stress is released mechanically by grinding, etching, cracking etc., spontaneous transformation occurs, at room temperature, of the left metastable high cristobalite crystals. This fact is interesting in connection with the conclusions drawn in section 4.2 about the preordered regions. In spite of the fact that not less than 70 hours are needed for the production of crystals of a few microns in size at $1480^\circ C$, and that impurity inclusions are necessary to form a stable nucleus, a certain relation to the concept of the preordered regions will not to be rejected.

Another fact is important in connection with table 2 and with the intrinsic

crystal growth rate. At a temperature of 1486°C a growth rate of 0.02 $\mu\text{m}/\text{min}$ occurs and an activation energy very similar to that of viscosity (see section 5.4.)¹⁴⁴). This indicates, that even in vacuo very small quantities of impurity cannot be totally excluded. A further fact is, that the growth rate is linear with time, although an electrically melted silica glass of type I (oxygen deficiency) was used; this shows the overwhelming effect of the presence of oxygen on surface crystallization for type I silica glasses.

The crystallization of pure silica glass to tridymite or quartz under normal atmospheric conditions has not yet been observed. The tridymite transformation above 870°C and the quartz transformation below 870°C is only possible in the presence of mineralizers^{1,146}).

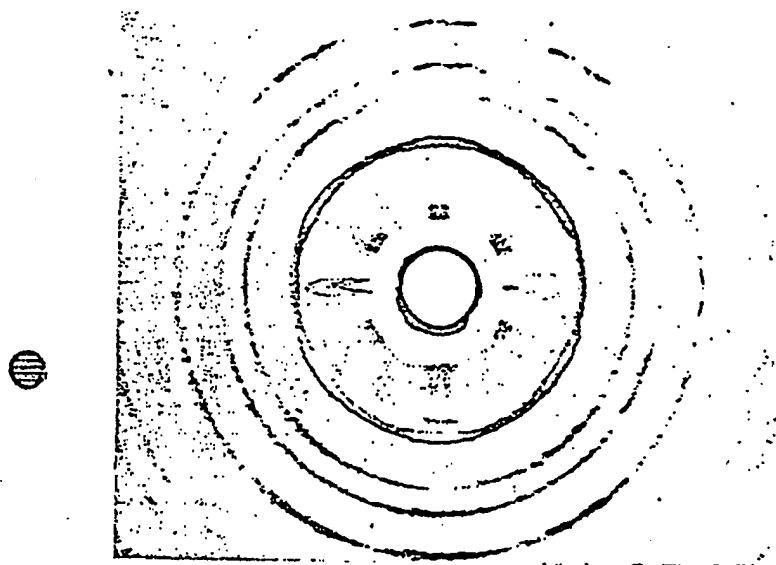
Under the action of high pressure the high pressure modifications of silica are obtained: keatite, coesite (above 20–40 kbar), and stishovite (above 97–130 kbar). A complete phase diagram is recently presented¹⁴⁷) including quartz, cristobalite, tridymite, coesite and stishovite.

A remarkable fact is, that the transformation under pressure to quartz and to coesite from silica glass is again dependent on water content of the surrounding atmosphere and of the compressed silica glass sample, and on the OH-content in the silica glass sample¹⁴⁸). As a result, at a temperature of 500°C and a pressure of 40 kbar, the rate of crystallization to quartz and coesite decreases in the series: silica gel \rightarrow GE 204 (wet loading) \rightarrow GE 204 and spectroil (air loading) \rightarrow spectroil (dry loading) \rightarrow GE 204 (dry loading) \rightarrow GE 204 (ultra-dry loading). The difference between the higher crystallization rate, of the "water"-rich sample spectroil and that of the "water"-poor sample GE 204 on the one hand, and the difference between the higher crystallization rate in water vapour and the lower one in dry atmosphere on the other hand, gives rise to the conclusion that water vapour and OH content have a catalytic influence on the crystallization mechanism. It is suggested, that a possible existence of a water-rich region in the vicinity of the interface should be responsible for this behaviour¹⁴⁸). Both these effects, the catalytic influence and the water-rich region, should be enhanced by pressure.

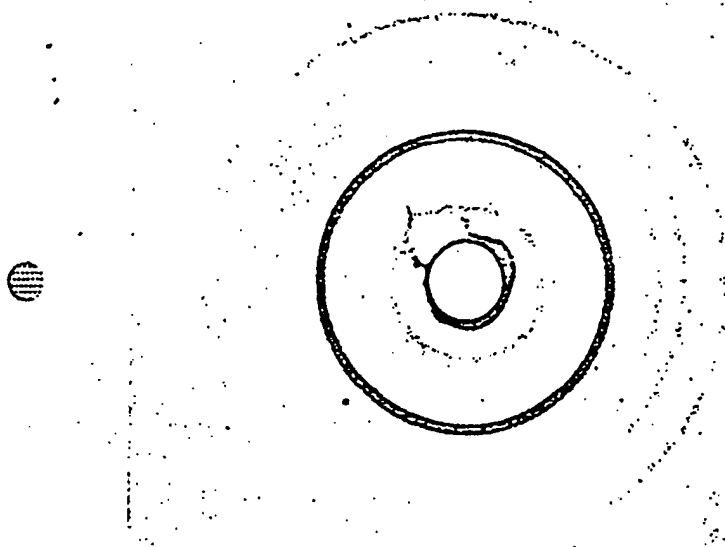
Preferred orientation of cristobalite crystallization on the surface of vitreous silica was observed in two cases.

First, the devitrified surface of a silica glass plate heated at 1200°C for 6 hours shows a habit plane or an orientation to some degree with respect to the surface, but only for the (101) planes of the low-temperature cristobalite, whereas, a completely random orientation is found for the other major α -cristobalite planes (111), (102) and (200)¹⁴⁹).

Second, silica glass fibers, when crystallized at 1200 or 1300°C, show preferred orientation of high- and also of low-temperature cristobalite (fig. 35a). This is only the case if the fibers were fresh and not annealed before



(a)



(b)

Fig. 35. Crystallization of silica glass fibers; (a) crystallized at 1270°C without annealing before crystallization; (b) crystallized at 1270°C after annealing at 1000°C.

crystallization, because annealing causes structural regroupings and a loss of the glass fiber anisotropy. Therefore no preferred orientation of the crystallized fiber is detectable when a 10 hours annealing at 1000°C preceded the crystallization (fig. 35b). This behaviour is regarded as an evidence that no surface-influenced crystallization leads to the texture effect as in the former case, but that the influence of the anisotropic structure of the silica glass fiber¹⁴⁰ gives rise to the oriented crystallization of the silica glass fiber to cristobalite.

References

- 1) R. B. Sosman, *The Phases of Silica* (Rutgers Univ. Press, New Brunswick, N.J., 1964).
- 2) G. Hetherington, K. H. Jack and M. W. Ramsay, *Phys. Chem. Glasses* 3 (1962) 129; 6 (1965) 6.
- 3) Trademark of W. C. Heraeus-Schott Comp., Germany, and Amersil Quartz Division, Engelhard Industries, Inc.
- 4) Trademark of Thermal Syndicate Ltd., England.
- 5) Trademark of General Electric Comp., U.S.A.
- 6) Trademark of Corning Glass Comp., U.S.A.
- 7) J. H. Rosolowski, *Am. Ceram. Soc. Bull.* (1966) 68, 381; Annual Meeting of the Am. Ceram. Soc.
- 8) P. Ehrenfest, *Commun. Kamerlingh Onnes Lab. Leiden Suppl.* 75b (1933).
- 9) E. Jenckel, Die glasige Erstarrung der Hochpolymere, in: *Die Physik der Hochpolymeren*, Vol. III, Ed. H. A. Stuart (Springer, Berlin, 1955) pp. 608-638;
F. Simon, *Z. Anorgan. Allgem. Chem.* 233 (1931) 219;
C. Tammann, *Der Glaszustand* (Leipzig, 1933);
R. Haase, *Thermodynamik der Mischphasen* (Springer, Berlin, 1956).
- 10) J. H. Gibbs, Nature of the Glass Transition and the Vitreous State, in: *Modern Aspects of the Vitreous State*, Vol. I, Ed. J. D. Mackenzie (Butterworth, London, 1960) p. 152;
J. H. Gibbs and E. A. DiMarzio, *J. Chem. Phys.* 28 (1958) 373.
- 11) R. W. Douglas and J. O. Isard, *J. Soc. Glass Technol.* 35 (1951) 206.
- 12) R. Brückner, *Glastech. Ber.* 37 (1964) 459.
- 13) B. E. Warren, *Z. Krist.* 86 (1933) 349.
- 14) B. E. Warren, H. Krutter and O. Morningstar, *J. Am. Ceram. Soc.* 19 (1936) 202.
- 15) B. E. Warren and J. Biscoe, *J. Am. Ceram. Soc.* 21 (1938) 49.
- 16) W. O. Milligan, H. A. Levy and S. W. Peterson, *Phys. Rev.* 83 (1951) 226.
- 17) J. Zarzycki, in: *Compt. Rend. I Ve Congr. Intern. du Verre*, Paris, 1956, p. 323.
- 18) J. T. Randall, H. P. Rooksby and B. S. Cooper, *J. Soc. Glass Technol.* 14 (1930) 219.
- 19) G. Hartleif, *Z. Anorgan. Allgem. Chem.* 238 (1938) 353.
- 20) E. A. Porai-Koshits, in: *Structure of Glass* (Acad. Sci. U.S.S.R., Moscow, 1960) (Transl. 1960) pp. 9-16.
- 21) R. J. Breen and A. H. Wever, Glass Structure Research Fellowship, St. Louis Univ. Rept. July 1, 1952.
- 22) E. Lorch, *Brit. J. Phys. C (Solid State Phys.)* 2 (1969) 229.
- 23) W. H. Zachariassen, *J. Am. Chem. Soc.* 54 (1932) 3841; *Glastech. Ber.* 11 (1933) 120.
- 24) A. Dietzel, *Glastech. Ber.* 22 (1948) 41, 81, 212.
- 25) J. M. Stevels, *Progress in the Theory of the Physical Properties of Glass* (Elsevier, Amsterdam, 1948).
- 26) J. M. Stevels, *Glass Ind.* 35 (1954) 69, 100, 102, 135, 160.
- 27) J. M. Stevels, *Philips Techn. Rev.* 22 (1960/61) 300, 337.
- 28) K. H. Sun, *J. Am. Ceram. Soc.* 30 (1947) 277.

- 29) M. L. Huggins, *J. Am. Ceram. Soc.* 38 (1955) 172.
- 30) A. A. Lebedev, *Tr. Gos. Optich. Inst. Leningrad* : (1921) No. 10; *Bull. Acad. Sci. USSR, Sci. Phys.* 4 (1940) 584.
- 31) O. A. Botvinkin, in: *Compt. Rend. 11^e Congr. Intern. du Verre*, Paris, 1956, p. 451.
- 32) W. Vogel and K. Gerth, *Glastech. Ber.* 31 (1958) 15.
- 33) W. Vogel, *Silikat Tech.* 10 (1959) 241; *Proc. All-Union Conf. Glassy State Leningrad* 3 (1959) 17.
- 34) W. Vogel and H. G. Byhan, *Silikat Tech.* 15 (1965) 212, 239.
- 35) J. W. Cahn and J. E. Hilliard, *J. Chem. Phys.* 31 (1959) 688.
- 36) J. W. Cahn, *J. Chem. Phys.* 42 (1965) 93.
- 37) W. B. Hillig, in: *Symp. Nucleation and Crystallization in Glasses and Melts*, Toronto, 1961 (Ceramic Soc., Columbia, Ohio, 1962) p. 78.
- 38) J. W. Cahn and R. J. Charles, *Phys. Chem. Glasses* 6 (1965) 181.
- 39) D. Turnbull, *J. Phys. Chem.* 66 (1962) 609; *J. Appl. Phys.* 21 (1950) 1022.
- 40) D. Turnbull, in: *Symp. Nucleation and Crystallization of Glasses and Melts*, Toronto, 1961 (Ceramic Soc., Columbia, Ohio, 1962) p. 75.
- 41) R. J. Charles, *J. Am. Ceram. Soc.* 46 (1963) 235; 47 (1964) 559; 49 (1966) 55.
- 42) L. W. Tilton, *J. Res. Natl. Bur. Std.* 59 (1957) 139.
- 43) H. A. Robinson, *J. Phys. Chem. Solids* 26 (1965) 209.
- 44) R. J. Bell and P. Dean, *Nature* 212 (1966) 1354.
- 45) R. J. Bell, N. F. Bird and P. Dean, *Brit. J. Phys. C (Proc. Phys. Soc.)* [2] 1 (1968) 299.
- 46) A. Smekal, *Novo Acta Leopoldina NF* 11 (1942).
- 47) A. Smekal, *Glastech. Ber.* 22 (1949) 278; *J. Soc. Glass Technol.* 35 (1951) 411.
- 48) K. Grjotheim and J. Krogh-Moe, *Glastek. Tidskr.* 11 (1956) 47.
- 49) A. Winter, *J. Am. Ceram. Soc.* 40 (1957) 54.
- 50) W. Noll, *Naturwissenschaften* 49 (1962) 505; *Angew. Chem.* 75 (1963) 123.
- 51) A. Dietzel, *Z. Elektrochem.* 48 (1942) 9.
- 52) W. A. Weyl, *J. Soc. Glass Technol.* 35 (1951) 421; *Glastech. Ber.* 30 (1957).
- 53) W. A. Weyl and E. Ch. Marboe, *The Constitution of Glasses; A Dynamic Interpretation*, Vols. 1 and 2 (Wiley-Interscience, New York, 1962, 1965).
- 54) H. Krebs, *Angew. Chem.* 70 (1958) 615; 78 (1966) 577.
- 55) V. Garino-Canina, *Verres Réfractaires* 10 (1956) 63, 151.
- 56) T. Bell, G. Hetherington and K. H. Jack, *Phys. Chem. Glasses* 3 (1962) 141.
- 57) A. J. Cohen, *Phys. Rev.* 105 (1957) 1151.
- 58) A. J. Cohen, *J. Chem. Phys.* 23 (1955) 765.
- 59) J. S. van Wieringen and A. Kats, *Philips Res. Rept.* 12 (1957) 423.
- 60) R. A. Weeks and E. Lell, *J. Appl. Phys.* 35 (1964) 1932.
- 61) J. M. Stevels, *Glastech. Ber.* 32 (1959) 307; *Philips Res. Rept.* 11 (1956) 103; in: *NonCrystalline Solids*, 1958, Ed. V. D. Fréchet (Wiley, New York, 1960) pp. 412-448.
- 62) R. Yokota, *Phys. Rev.* 91 (1953) 1913.
- 63) M. Lautout, *J. Chim. Phys.* 52 (1955) 169.
- 64) S. Cohen, *Bull. Soc. Franc. Ceram. No.* 56 (1962) 29; *Verres Réfractaires* 23 (1969) 189.
- 65) A. J. Harrison, *J. Am. Ceram. Soc.* 30 (1947) 362.
- 66) H. Scholze, *Glastech. Ber.* 32 (1959) 81, 142.
- 67) E. R. Lippincott, A. van Valkenburg, Ch. E. Weir and E. N. Bunting, *J. Res. Natl. Bur. Std.* 61 (1958) 61.
- 68) J. Zarzycki and F. Naudin, *Verres Réfractaires* 14 (1960) 1.
- 69) P. H. Gaskell, *Trans. Faraday Soc.* 62 (1966) 1493, 1505.
- 70) R. Brückner, *Glastech. Ber.* 37 (1964) 500.
- 71) P. H. Gaskell and F. J. Grove, in: *Compt. Rend. VII^e Congr. Intern. du Verre*, Brussels, 1965, No. 363.
- 72) H. Mohn, in: *60 Jahre Quarzglas, 25 Jahre Hochvakuumtechnik*, Ed. W. C. Heraeus (1961) pp. 105-130.

- 73) G. Hetherington and K. H. Jack, *Phys. Chem. Glasses* 3 (1962) 129.
- 74) H. Scholze, H. Franz and L. Merker, *Glastech. Ber.* 32 (1959) 421.
- 75) R. Brückner, *Glastech. Ber.* 37 (1964) 459; 38 (1965) 153.
- 76) W. Poch, *Glastech. Ber.* 37 (1964) 533.
- 77) H. Scholze, *Glas-Email-Keramo-Tech.* 19 (1968) 389.
- 78) A. Winter and M. J. Cabannes, *Compt. Rend. (Paris)* 240 (1955) 2397.
- 79) H. Rau, in: *60 Jahre Quarz-glas, 25 Jahre Hochvakuumtechnik*, Ed. W. C. Heraeus (1961) pp. 77-104.
- 80) V. Garino-Canina, *Rev. Opt. Théor. Instr.* 34 (1955) 323.
- 81) J. F. Bacon, A. A. Hasapis and J. W. Wholley, *Phys. Chem. Glasses* 1 (1960) 90.
- 82) W. H. Keesom and D. W. Doborzynski, *Physica* 1 (1934) 1058.
- 83) H. T. Smyth, *J. Am. Ceram. Soc.* 38 (1955) 140.
- 84) R. Brückner, *Glastech. Ber.* 37 (1964) 536.
- 85) J. I. Frenkel, *Statistische Physik* (Akademie-Verlag, Berlin, 1957) ch. IX;
J. I. Frenkel, *Theory of Fluids* (Akademie-Verlag, Berlin, 1957) ch. VII.
- 86) M. Volmer and A. Wever, *Z. Physik. Chem.* 119 (1926) 277.
- 87) J. C. Fischer, J. H. Hollomon and D. Turnbull, *J. Appl. Phys.* 19 (1948) 775.
- 88) P. W. Bridgman, *Am. J. Sci.* 10 (1925) 359.
- 89) J. Reitzel, J. Simon and J. A. Walker, *Rev. Sci. Instr.* 28 (1957) 828.
- 90) C. L. Babcock, S. W. Barber and K. Fajans, in: *III Congr. Intern. de Vetro, Venezia*, 1953, p. 202.
- 91) F. Birch and R. B. Dow, *Bull. Geol. Soc. Am.* 47 (1936) 1235.
- 92) K. Vedam, E. D. D. Schmidt and R. Roy, *J. Am. Ceram. Soc.* 49 (1966) 531.
- 93) H. Mueller, *Physica* 6 (1935) 179.
- 94) J. D. Mackenzie, *J. Am. Ceram. Soc.* 46 (1963) 461, 470.
- 95) R. Roy and H. M. Cohen, *Nature* 190 (1961) 789; *Phys. Chem. Glasses* 6 (1965) 149.
- 96) E. B. Christiansen, S. S. Kistler and W. B. Gogartz, *J. Am. Ceram. Soc.* 45 (1962) 172.
- 97) P. W. Bridgman and J. Simon, *J. Appl. Phys.* 24 (1953) 405;
J. Arndt, *J. Am. Ceram. Soc.* 52 (1969) 285.
- 98) R. M. Kimmel and D. R. Uhlmann, *Phys. Chem. Glasses* 10 (1969) 12.
- 99) J. Arndt and D. Stöffler, *Phys. Chem. Glasses* 10 (1969) 117;
D. Stöffler and J. Arndt, *Naturwissenschaften* 56 (1969) 100.
- 100) J. D. Mackenzie, *J. Am. Ceram. Soc.* 47 (1964) 76.
- 101) H. T. Smyth, J. W. Londree and G. E. Lorey, *J. Am. Ceram. Soc.* 36 (1953) 238.
- 102) H. T. Smyth, *J. Am. Ceram. Soc.* 42 (1959) 276.
- 103) F. P. Mallinder and B. A. Proctor, *Phys. Chem. Glasses* 5 (1964) 91.
- 104) W. B. Hillig, in: *Symposium sur la Résistance Mécanique du Verre et les Moyens de l'Améliorer*, Florence, 1961 (Union Scientifique Continentale du Verre, Charleroi, Belgium, 1962) pp. 1-1/1-31.
- 105) J. W. Marx and J. M. Sivertsen, *J. Appl. Phys.* 24 (1953) 81.
- 106) H. J. McSkimin, *J. Appl. Phys.* 24 (1953) 988.
- 107) M. E. Fine, H. van Duyn and N. T. Kenney, *J. Appl. Phys.* 25 (1954) 402.
- 108) E. Deeg, *Glastech. Ber.* 31 (1958) 124;
S. Spinner and G. W. Cleek, *J. Appl. Phys.* 31 (1960) 1407.
- 109) G. J. Dienes, *J. Phys. Chem. Solids* 7 (1958) 290.
- 110) O. L. Anderson and G. J. Dienes, in: *Non-Crystalline Solids*, 1958, Ed. V. D. Fréchet (Wiley, New York, 1960) pp. 449-490.
- 111) D. B. Fraser, *J. Appl. Phys.* 39 (1968) 5868.
- 112) O. L. Anderson and H. E. Bömmel, *J. Am. Ceram. Soc.* 38 (1955) 125.
- 113) J. T. Krause, *J. Am. Ceram. Soc.* 47 (1964) 103.
- 114) R. E. Strakna and H. T. Savage, *J. Appl. Phys.* 35 (1964) 1445.
- 115) C. R. Kurkjian and J. T. Krause, *J. Am. Ceram. Soc.* 49 (1966) 134.
- 116) H. T. Smyth, H. S. Skogen and W. B. Harsell, *J. Am. Ceram. Soc.* 36 (1953) 327.
- 117) R. B. Sosman, *The Properties of Silica* (The Chemical Catalog Comp., New York, 1927) p. 313.

- 118) W. Geffcken and N. Neuroth, *Glastech. Ber. Sonderband* 32K (1959) V/48-53.
- 119) O. L. Anderson, *J. Phys. Chem. Solids* 12 (1959) 41.
- 120) M. Born and K. Huang, *Dynamic Theory of Lattices* (Oxford Univ. Press, 1954) ch. 3.
- 121) P. Fulbacher, A. J. Leadbetter, J. A. Morrison and B. P. Stoicheff, *J. Phys. Chem. Solids* 12 (1959) 53;
A. J. Leadbetter, *J. Chem. Phys.* 51 (1969) 779.
- 122) St. M. Shapiro, R. W. Gammon and H. Z. Cummins, *Appl. Phys. Letters* 9 (1966) 157
- 123) J. M. Stevels, in: *Encyclopedia of Physics*, Vol. 13, Ed. S. Flügge (Springer, Berlin, 1962) p. 577.
- 124) C. Kittel, *Phys. Rev.* 75 (1949) 972.
- 125) P. G. Klemens, in: *Non-Crystalline Solids*, 1958, Ed. V. D. Fréchet (Wiley, New York, 1960) pp. 508-528.
- 126) W. D. Kingery, *J. Am. Ceram. Soc.* 38 (1955) 251; 44 (1961) 302.
- 127) K. L. Wray and T. J. Connolly, *J. Appl. Phys.* 30 (1959) 1702.
- 128) E. H. Ratchiff, *Brit. J. Appl. Phys.* 10 (1951) 108.
- 129) P. G. Klemens, *Proc. Roy. Soc. (London) A* 208 (1951) 108.
- 130) R. Berman, *Proc. Roy. Soc. (London) A* 208 (1951) 90.
- 131) P. G. Klemens, J. G. Castle and D. W. Feldman, *Phys. Chem. Glasses* 2 (1964) 104.
- 132) J. G. Morley, P. A. Andrews and J. Whetney, *Phys. Chem. Glasses* 5 (1964) 1.
- 133) B. A. Proctor, I. Whitney and J. W. Johnson, *Proc. Roy. Soc. (London) A* 297 (1967) 534.
- 134) R. J. Charles and W. B. Hillig, in: *Symposium sur la Résistance Mécanique du Verre et les Moyens de l'Améliorer*, Florence, 1961 (Union Scientifique Continentale du Verre, Charleroi, Belgium, 1962) pp. 11-3/1-17.
- 135) J. B. Murgatroyd, *J. Soc. Glass Technol.* 28 (1944) 368, 388.
- 136) S. Bateson, *J. Soc. Glass Technol.* 37 (1953) 302.
- 137) W. F. Thomas, *Nature* 181 (1958) 1006; *Phys. Chem. Glasses* 1 (1960) 4.
- 138) W. H. Otto, *J. Am. Ceram. Soc.* 44 (1961) 68.
- 139) L. Merker, in: *Symposium sur la Résistance Mécanique du Verre et les Moyens de l'Améliorer*, Florence, 1961 (Union Scientifique Continentale du Verre, Charleroi, Belgium, 1962) pp. 567-687.
- 140) R. Brückner, in: *Compt. Rend. VII Congr. Intern. du Verre*, Brussels, 1965 No. 38/1-12, 1.3.2.
- 141) F. E. Wagstaff, S. D. Brown and I. B. Cutler, *Phys. Chem. Glasses* 5 (1964) 76.
- 142) F. E. Wagstaff and K. J. Richards, *J. Am. Ceram. Soc.* 48 (1965) 382; 49 (1966) 118.
- 143) J. Hlavac and L. Vaskova, *Silicaty* 9 (1965) 237.
- 144) F. E. Wagstaff, *J. Am. Ceram. Soc.* 51 (1968) 449.
- 145) A. Dietzel and H. Wickert, *Glastech. Ber.* 29 (1956) 1.
- 146) O. W. Flörke, *Ber. Deut. Keram. Ges.* 38 (1961) 89.
- 147) D. Stöffler and J. Arndt, *Naturwissenschaften* 56 (1969) 100.
- 148) D. R. Uhlmann, J. F. Hays and D. Turnbull, *Phys. Chem. Glasses* 7 (1966) 159.
- 149) R. F. Hochman and J. D. Fleming, *J. Am. Ceram. Soc.* 47 (1964) 104.